Natalia Sinelnikova

SYNTHESIS OF NEW INHIBITORS OF HUMAN HOMOGENTISATE 1,2-DIOXYGENASE, ONE OF THE ENZYMES, INVOLVED IN TYROSINE METABOLIC PATHWAY IN HUMANS

Mémoire présenté
à la Faculté des études supérieures de l'Université Laval
dans le cadre du programme de maîtrise en chimie
pour l'obtention du grade de maître ès sciences (M.Sc.)

DÉPARTEMENT DE CHIMIE
FACULTÉ DES SCIENCES ET DE GÉNIE
UNIVERSITÉ LAVAL
QUÉBEC

2006

Résumé

La tyrosinémie héréditaire de type I (TH I) est une maladie génétique. Elle est causée par une activité réduite de *la fumarylacétoacétate hydrolase* (FAH), la dernière enzyme impliquée dans la dégradation de la tyrosine chez l'humain. Cette déficience enzymatique cause l'accumulation de produits toxiques dans l'organisme, ce qui occasionne de graves problèmes de foie et une issue fatale dans l'enfance.

La tyrosinémie héréditaire est une maladie rare. L'incidence de cette maladie dans le monde est une personne sur 120 000 naissances vivantes. Par contre, dans les régions du Saguenay Lac Saint-Jean et de Charlevoix l'incidence de cette maladie est très élevée : une personne sur 1846 nouveau-nés.

Le but de ce projet est la synthèse des inhibiteurs de *l'homogentisate 1,2- dioxygénase* (HGO), la troisième enzyme, impliquée dans la dégradation de la tyrosine. Ces inhibiteurs représentent les analogues halogénés de l'acide homogentisique qui est le substrat de l'HGO.

L'utilisation de ces inhibiteurs dans le traitement de la tyrosinémie héréditaire de type I peut devenir une bonne alternative de la transplantation hépatique qui représente, en ce moment, la méthode la plus efficace pour traiter cette maladie.

Abstract

Hereditary tyrosinemia type (HT I) is the most severe genetic disease in human tyrosine catabolism, affecting liver, kidney and peripheral nerves. It results from reduced activity of *fumarylacetoacetate hydrolase* (FAH), the final enzyme in the degradation of tyrosine. The accumulation of toxic metabolites in liver leads to progressive liver malfunction and cirrhosis which leads to the fatal outcome in infancy.

Despite the fact that tyrosinemia type I is a rare genetic disease (the worldwide prevalence is 1 case to 120 000 newborns), in Saguenay Lac Saint-Jean and Charlevoix regions of Quebec the prevalence of tyrosinemia type I is very high, one case to 1846 newborns.

The object of this project is the synthesis of inhibitors of the *homogentisate 1,2- dioxygenase* (HGO), the third enzyme in the catabolic tyrosine pathway in human. These inhibitors represent the halogenated analogues of homogentisic acid, which is a substrate of HGO.

Treatment of HT I using these inhibitors may be a very good alternative to the orthotopic liver transplantation (OLT) which is now the only effective form of therapy of this disease.

Acknowledgements

First of all I would like to thank my professor, John Boukouvalas. Thanks to you I had a chance to touch again the organic chemistry, to feel it charm and complexity at the same time, to improve my knowledge and, sometimes, to open absolutely new and unknown sides of chemistry.

After that, I would like to thank all the members of our laboratory, namely, Jian-Xin Wang, Martin Pouliot, Olivier Marion and Paola Beltran for your presence and help, for your good mood and sense of humor. I address special thanks to Xue-Jing Zheng. I appreciate very much your help and your support especially at the beginning of my studies.

Next, I would like to thank my parents and my friends. Despite the fact that you live in the other end of the world, you are always with me in my heart and your sage counsels help me to survive the difficult moments in my life.

Finally, I would like to thank my husband Evgueni and my adorable son Sviatoslav for your love, kindness and support. You are an inexhaustible source for my inspiration.

Contents

List of Figures

List of Schemes

List of Tables

Abbreviations and Symbols

Products and Solvents

DIBAL-H	Diisobutylaluminium hydride
DMSO	Dimethylsulfoxide
Et	Ethyl
Hex	Hexane
Me	Methyl
Ms	Mesylate
Py	Pyridine
THF	Tetrahydrofuran

Units

Å	Angstrom
^{o}C	Degree Celsius
cm^{-1}	Reciprocal centimeters
equiv	Equivalent
g	Gram
h	Hour
Hz	Hertz
kJ	Kilojoule
M	Molar
MHz	Megahertz

min	Minute
mol	Mole
mol^{-1}	Reciprocal mole
μ	Micron
ml	Milliliter
nm	Nanometer
ppm	Unit of part per million

Methods of analyses

IR	Infrared
Mp	Melting point
^{1}H NMR	Proton Nuclear Magnetic Resonance
^{13}C NMR	Carbon Nuclear Magnetic Resonance
R_f	Retention factor
TLC	Thin Layer Chromatography
UV	Ultra-violet

NMR Symbols

δ	Chemical shift in ppm
d	Doublet
dd	Doublet of doublet
J	Coupling constant
s	Singlet

Introduction

Every human body cell carries 23 pairs of chromosomes. Chromosomes are long strands of DNA which incorporate the genes. These genes contain the unique information of human which allows to human body function correctly. So, when a gene is missing or not functioning properly, a genetic disease will result. Now there are more that 4 000 genetic diseases. Most of them arise from the deficiency of the enzyme involved in essential amino acid catabolic pathway. The hereditary tyrosinemia type I is a good example of the disease concerned with metabolism of tyrosine.

L-tyrosine is a nonessential amino acid commonly found in animal and vegetable proteins. It can be synthesized in the body from phenylalanine. As a building block for several important brain chemicals, *L*-tyrosine is needed to make the adrenal hormones epinephrine, norepinephrine serotonin and dopamine, all of which work to regulate mood. *L*-tyrosine is also aids in the production of melanin, the skin and hair pigment, and in the function of organs in the body responsible for making and regulating hormones, including adrenal, thyroid, thyroxin and pituitary glands. *L*-tyrosine is also involved in the synthesis of enkephalins, substances that have pain relieving effects in the body.

The metabolism of *L*-tyrosine in human takes place primordially in liver and five enzymes catalyze this process (**Figure 1**).[1]

The first step of tyrosine metabolism is the oxidation of tyrosine to obtain *p*-hydroxyphenylpyruvic acid (*p*-HPPA).[2] This reaction needs the enzyme *tyrosine aminotransferase* and the vitamin B_6. The second enzyme, *p-hydroxyphenylpyruvate dioxygenase* (*p*-HPPD), controls a very complicated reaction inclusive the chain change of the benzene nucleus to obtain homogentisic acid. This process is irreversible in the humans and needs the vitamin C as a "red ox" agent to stabilize the enzyme.

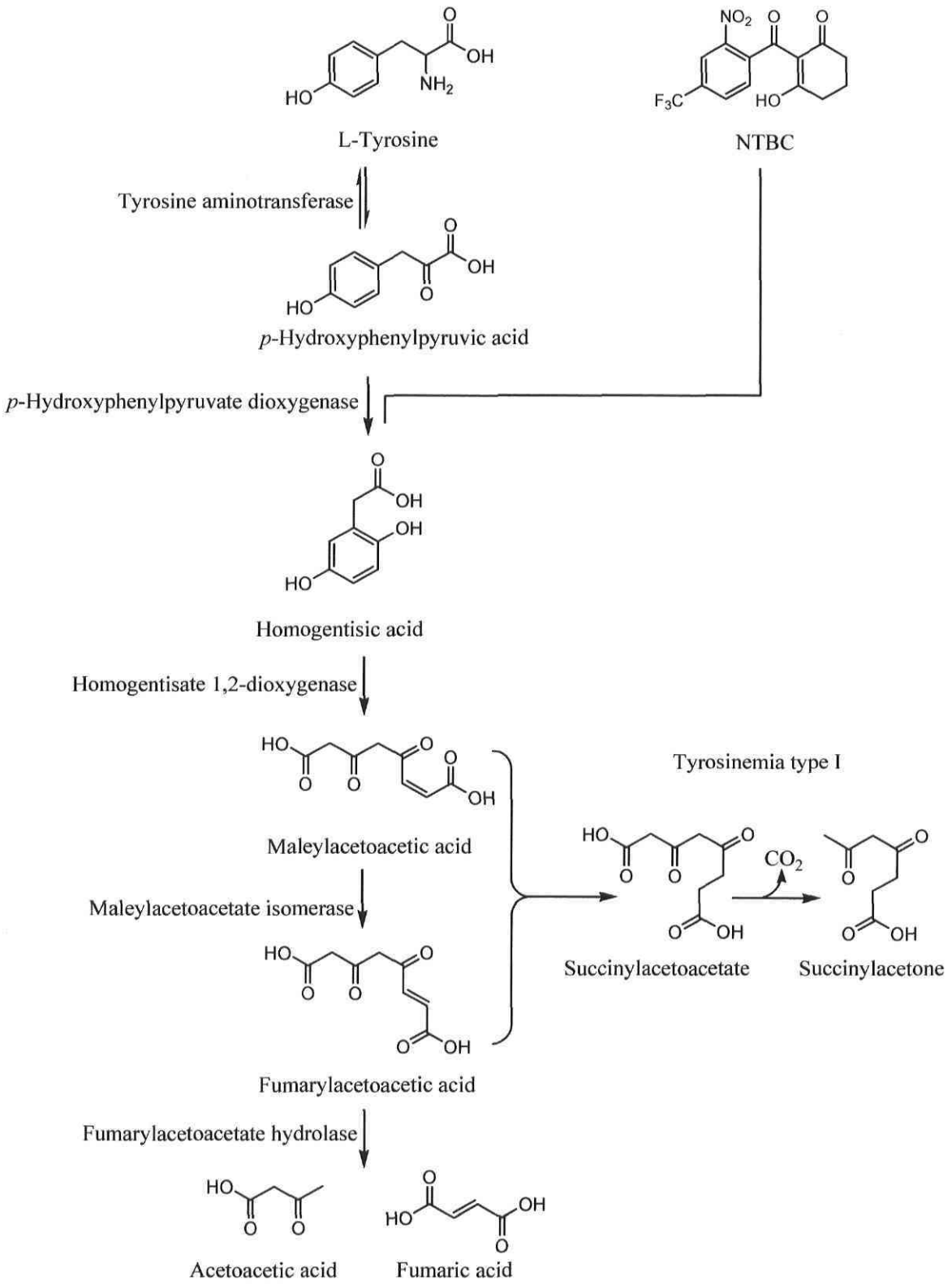

Figure 1. The metabolic pathway of tyrosine.

The third enzyme, *homogentisate 1,2-dioxygenase*, breaks the benzene nucleus of homogentisic acid to obtain maleylacetoacetic acid. This step is irreversible and needs the presence of glutathione (GSH) and vitamin C.

The before last step of the tyrosine metabolism is the maleylacetoacid isomerization to obtain fumarylacetoacetic acid. This step is irreversible and realized by the enzyme *maleylacetoacetate isomerase* in the presence of GSH as a co-factor.

Finally, the last enzyme, *fumarylacetoacetate hydrolase* (FAH), transforms fumarylacetoacetic acid in two small products: fumaric acid and acetoacetic acid which then can be eliminated from the body.

Thus, for the appropriate passing of tyrosine metabolism in the human body it is necessary to not have any mutations or activity deficient of the five enzymes. An enzyme deficiency in any of steps of this metabolic pathway causes in humans a known metabolic disease.

For example, the tyrosinemia type II (oculocutaneous tyrosinemia) is an autosomal recessive disorder affecting the eyes, skin and central nervous system.[3] It is due to a deficiency of the enzyme *tyrosine aminotransferase*.

Tyrosinemia type III, caused by deficiency of *p-hydroxyphenylpyruvate dioxygenase*, is a very rare disease which leads to the severe mental retardation and neurological abnormalities such as convulsion and ataxia.[4, 5]

The deficiency of the enzyme *homogentisate 1,2-dioxygenase* is the reason of the rare hereditary disorder known as alkaptonuria, characterized by a type of arthritis.[6]

In the meantime, there is one more type of tyrosine metabolic disease. It is question of hereditary tyrosinemia type I (HT I, hepatorenal tyrosinemia).[7]

Hereditary tyrosinemia type I is the most severe disease in human tyrosine metabolism, affecting liver, kidney, and peripheral nerves. HT I results from reduced activity of *fumarylacetoacetate hydrolase* (FAH), the final enzyme in the degradation of tyrosine. It is generally accepted that fumarylacetoacetate and its spontaneous reaction product, succinylacetone (the diagnostic compound of the disease), are toxic due to their considerable reactivity with key cellular molecules. The accumulation of these products in

liver leads to progressive liver malfunction and cirrhosis in infancy and hepatocellular carcinoma develops in many patients by mid-childhood. Patients may also have renal tubular damage and acute neurological crises like those of porphyria.[8] The hereditary tyrosinemia type I is an autosomal recessive disease. It is inherited in an autosomal recessive fashion which means that in order to have the disease a child must inherit two defective genes, one from each parent. In families where both parents are carriers of the gene for the disease, there is a one in four risk that a child will have tyrosinemia. Tyrosinemia type I is a rare disease. The worldwide prevalence varies from one case in *100 000* to one case in *120 000* newborns. However, in Quebec region the prevalence of this disease reaches one case in 17 000 live births and, particularly, in Saguenay Lac Saint-Jean and Charlevoix regions, the prevalence of tyrosinemia type I is very high, one case in 1 846 newborns. In these regions one person from 20 is a carrier of the deficient gene. That means that if both parents have the deficient gene, the risk to have a diseased child reaches 25% in the ever pregnancy.[9] This high prevalence of tyrosinemia type I is explained by the so-called the *founder effect,* which is the result of French colonization of Canada.[10]

The founder effect occurs when populations are started from a small number of pioneer individuals of an original population. Due to small sample size, the new population could have a much different genetic ratio than the original one. A few dozen families, who migrated north from Charlevoix Country in Quebec, settled the Chicoutimi region in 1840s. After settled this area, few settlers followed, and most of people there are the descendent of those original families. The pedigrees of all patents could be traced back to just one couple, Louise Gagné and his wife, Mary Michel, who immigrated to Quebec from France in mid-seventeenth century. It is obvious that either Louis or Mary had the gene for tyrosinemia. Since only small number of people migrated into Chicoutimi, those residents are rather inbred. Thus, tyrosinemia-coded gene was shared in this region.

Tyrosinemia type l was first described by Baber in 1956.[11, 12] Around 1964, a group of physicians in the Chicoutimi area of Quebec Province became aware of an increased incidence of lethal infantile cirrhosis in this region.

In 1965, pediatrician Dr. Jean Larochelle, who discovered the tyrosinemia in this region, reported 29 such cases; 14 cases were the familial ones. In 1967 La Du showed a deficiency of *p*-hydroxyphenylpyruvic acid (*p*-HPPA) in the liver of such patients.

The clinical features of the tyrosinemia type I tend to fall into two categories: an acute form and a chronic form.[13] In the acute form, affected individuals present very early in infancy with failure to thrive, vomiting, jaundice, hepatomegaly and, often, a cabbage-like odor. In the chronic form, so-called "Baber's syndrome", affected individuals present with failure to thrive, hepatomegaly, vitamin D-resistant rickets, renal Fanconi syndrome, and episodes of a porphyria-like illness characterized by vomiting, abdominal pain and neurological abnormalities, including inability to walk and outright paralysis. Despite of vigorous therapy, most of the infants, affected with acute form of tyrosinemia, die between three and nine months of age from acute liver failure. Progressive chronic liver disease leading to cirrhosis results in death before the end of the second decade of life.

Today there are three main forms of treatment for tyrosinemia type I: adherence to a specialized diet, liver transplantation and medication.[14] For years, tyrosinemia type I has been treated by a strict, low protein diet that has low levels of tyrosine, phenylalanine and methionine. Adherence of this diet may lead to an improvement of symptoms and a slow progression of the disorder. However, the serious complication such as liver failure may still occur and it is impossible to prevent the fatal outcome. The second form of treatment, liver transplantation, is the most effective and only definitive form of therapy at the present time because it cures the disease and prevents neurological crisis. Now it is possible to do orthotopic liver transplantation (OLT) at an early stage (before 1 year of age), which enables patients with tyrosinemia type I to survive and normalizes the hepatic tyrosine metabolism. However, the prognosis of the disease in extra hepatic organs remains unknown.[15, 16] Furthermore, urinary succinylacetone excretion continues in the majority of patients what means that the enzyme defect persists in the kidneys and the disease can progress again. Finally, OLT is accompanied by immunosuppressive therapy for the rest of life which can provoke cancerous diseases. It needs to add that this mode of therapy is very expensive.

In 1992 Lindstedt and associates developed a new method of treatment for the tyrosinemia type I, namely, inhibition of one the enzymes involved in tyrosine catabolic pathway.[17] They found that *p-hydroxyphenylpyruvate dioxygenase* (*p*-HPPD), the second enzyme involved in tyrosine catabolic pathway, is efficiently inhibited by 2-(2-nitro-4-trifluoromethylbenzoyl)-1,3-cyclohexanedione (NTBC) (**Figure 2**). NTBC is the competitive reversible inhibitor with IC_{50}=40nM. Inhibition of *p*-HPPD may prevent the development of cirrhosis and abolish or diminish the risk of liver cancer. From 220 patients who began the drug in infancy, 88% have survived for years. That is far better than the normal 29% survival rate with diet alone. Of the 101 patients aged 2 to 8 years who had started NTBC treatment before 2 years of age, no patients developed cancer after 2 years of age.[18]

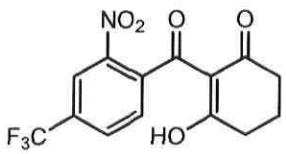

NTBC

2-(2-nitro-4-trifluoromethylbenzoyl)-1,3-cyclohexanedione

Figure 2. Inhibitor of *p*-hydroxyphenylpyruvate dioxygenase, *p*-HPPD.

However, NTBC does not work for everyone and is not a cure. Even in patients that the drug helped, no one yet knows if taking NTBS for life could keep the disease at bay or if eventually they would need a liver transplant. Studies to determine that are continuing. Furthermore, cancerous nodules develop in the mice despite NTBC treatment at birth. These studies suggest that NTBC may not prevent hepatocellular carcinoma.[19]

Since 1965, 185 cases of the tyrosinemia type I has been reported.[9] Every year from 2 to 3 newborns in Quebec region have this anomaly. Today there are several methods to reveal this disease. One of them is the amniocentesis, i.e. the analysis of amniotic fluid between the 13th and 16th weeks of the pregnancy.

The other one is the porter test. It has been developed by the scientists of Laval University (group of Tanguay R. M.) and Oregon Health Sciences University. This test allows to identify the persons who might have the gene causing the tyrosinemia type I. The next step in treatment of tyrosinemia type I is the so-called gene therapy. It is a question of the removal of deficient gene and incorporation of good one.

However, the search and development of the inhibitors of one of the enzymes involved in catabolic tyrosine pathway is always of current importance since it could represent a good alternative to liver transplantation, greatly improve the health state of the patients with hereditary tyrosinemia type I or even heal this severe disease.

Chapter 1

Introduction to Enzymes

1.1 Classification of Enzymes

Living organisms possess complex network of chemical reactions and each of these reactions is controlled by an enzyme.[20] Enzymes increase the rate of chemical reactions taking place within living cells without themselves suffering any overall change. Like any catalyst, enzymes work by lowering the activation energy of a reaction, thus allowing the reaction to proceed to its steady state or completion much faster than it otherwise would. Enzymes are necessary within biological cells because most chemical reactions required by the cell would occur too slowly to sustain life. Enzymes may speed up biochemical reactions by a factor of many thousand times. They remain unaltered by the completed reaction and can therefore continue catalysis.

There are more than 3000 known enzymes today. The International Enzyme Commission divided enzymes into six main classes, on the base of the total reaction catalyzed (**Table 1**).

Group Name	Type of Reaction Catalyzed
Oxidoreductases	Oxidation-reduction reactions
Transferases	Transfer of functional groups
Hydrolases	Hydrolysis reactions
Lyases	Addition to double bonds or its reverse
Isomerases	Isomerization reactions
Ligases or Synthetases	Formation of bonds with ATP cleavage

Table 1. IEC classification of enzymes.

1.2 Structure of Enzymes

All enzymes are proteins – macromolecules with molecular weights of at least several thousand Daltons. They are found in abundance in living organisms, making up more than half the dry weight of cells. All proteins consist of amino-acid units, joined in series. The sequence of amino-acids in protein is specific, being determined by the structure of the genetic material of the cell, and this gives each protein unique properties.

Proteins can be found in four different forms, or structures. The first is called **the primary structure**, which is described as long polypeptide chains. To form the polypeptide chain each amino acid is linked to the next via an amide bond, forming a linear sequence of 100-1000 amino acids. This sequence of amino acids forms the primary structure. The sequence of amino acids in the polypeptide chain is all-important because in contains all the information to confer both the three-dimensional structure of proteins in general, and the catalytic activity of enzymes in particular.

Secondary structure is the term given to local regions (10-20 amino acids) of stable, ordered three-dimensional structures held together by hydrogen bonding. There are at least three stable forms of secondary structure commonly observed in proteins: the α-helix, the β-sheet and the β-turn. The α-helix is the helical structure formed by a single polypeptide chain in which hydrogen bonds are formed between the carbonyl oxygen of one amide linkage and the N-H of the amide linkage four residues ahead in the chain, represented as NH···O=C. There are 3.6 amino acid residues per turn of the helix. In the α-helix, the amino acid R-groups protrude out from the helically coiled polypeptide backbone. The surface of the α-helix largely consists of the R-groups of amino acid residues (**Figure 3, a**). Another common secondary structure is the β-sheet. This is the structure formed by two or more linear polypeptide strands, held together by a series of interstrand hydrogen bonds. There are two types of β-sheet structures: parallel β-sheet, in which the peptide strands both proceed in the same amino-to-carboxyl direction; and anti-parallel, in which the peptide strands proceed in opposite direction. Because of the tetrahedral nature of carbon bonds, the β-sheet is puckered, leading to the designation pleated sheet. The N-H groups in the backbone of one strand establish hydrogen bonds with the C=O groups in the backbone of the adjacent, parallel strand. The cumulative effect of

multiple such hydrogen bonds arranged in this way contributes to the sheet's stability and structural rigidity and integrity. The α-C atoms of adjacent strands stand 0.35 nm (**Figure 3, b**). The β-turn is a structure often formed at the end of β-sheet which leads to a 180° turn in the direction of the peptide chain.

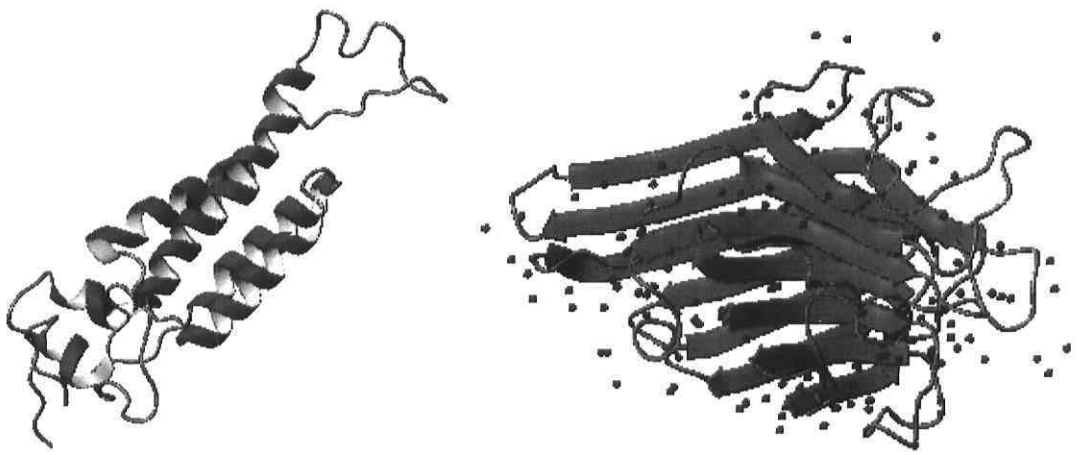

a) Tobacco Mosaic Virus coat protein (mostly α-helix protein).

b) Concanavalin A (mostly β-sheet protein).

Figure 3. The secondary structure of proteins

Tertiary protein structure refers to the complete three dimensional folding of a protein. Stabilization of a protein's tertiary structure may involve interactions between amino acids located far apart along the primary sequence. These may include weak interactions such as hydrogen bonds and Van der Waals interactions; ionic bonds involving negatively charged and positively charged amino acid side-chain groups; disulfide bonds, covalent linkages that may form as the thiol groups of two cysteine residues.

Quaternary protein structure refers to the regular association of two or more polypeptide chains to form a complex. A multi-subunit protein may be composed of two or more identical polypeptides, or it may include different polypeptides. Quaternary structure tends to be stabilized mainly by weak interactions between residues exposed on surfaces polypeptides within a complex.

1.3 Specificity of Enzyme Action

The main part of the enzyme protein responsible for catalysis is **the active site**. This comprises only a small proportion of the total volume of the enzyme and is usually at or near the surface, since it must be accessible to substrate molecules. The fit between the active site and the combined substrate molecule appears to be close over a patch of possibly up to 15-20 Å in diameter. Active site is responsible for the enzymatic properties of the molecule. It determines both the specificity and the catalytic activity. The binding and catalytic sites must be either amino-acid residues or cofactors, the latter being themselves bound to amino-acid side chains. The active site often includes both polar and non-polar amino-acid residues, creating an arrangement of hydrophilic and hydrophobic microenvironments not found elsewhere on an enzyme molecule. Thus, the function of an enzyme may depend not only on the spatial arrangement of binding and catalytic sites, but also on the environment in which these sites occur.

Specificity of the enzyme for the substrate depends on the nature of the active site. Enzymes differ in their degree of specificity. On the basis of specificity, the following classification of the enzymes is done:

1. **Absolutely specific enzymes** will act on a particular substrate only. For example, succinate dehydrogenase enzyme acts only on succinate.
2. **Nearly absolutely specific enzymes** are more or less specific in their substrate specificity but may deviant to some extent. For example, aspartase enzyme normally adds ammonia on fumarate but may also add on maleate.
3. **Absolutely stereospecific enzymes** are specific for a particular group of substrate but these should be only in the stereospecific form. For example, L-Amino acid oxidase can oxidize all the amino acids which are in L-configuration.
4. **Group specific enzymes** are having specificity for a particular group in the substrates. For example, acid phosphatase enzyme hydrolyzes the phosphoryl group from any phosphoryl ester.

1.4 Mechanism of Enzyme Action

In 1894 Emil Fischer suggested that enzyme specificity implied the presence of complementary structural features between enzyme and substrate: a substrate might fit into its complementary site on the enzyme as a key fits into a lock. According to **the lock-and-key model**, all structures remain fixed throughout the binding process.

Despite the fact that the lock-and-key model explains many features of enzyme specificity, it takes no account of the known flexibility of proteins. Nevertheless, X-ray diffraction analysis and data of nuclear magnetic resonance have revealed difference in structure between free and substrate-bound enzymes. Thus, the binding of a substrate to an enzyme may bring about a conformational change, i.e. a change in three-dimensional structure.

In 1958 Koshland suggested **the induced-fit hypothesis**. According to this hypothesis the structure of a substrate may be complementary to that of the active site in the enzyme-substrate complex, but not in the free enzyme: a conformational change takes place in the enzyme during the binding of substrate which results in the required matching of structures. The induced-fit hypothesis essentially requires the active site to be floppy and the substrate to be rigid, allowing the enzyme to wrap itself around the substrate, in this way bringing together the corresponding catalytic sites and reacting group. Such a mechanism could help to achieve a high degree of specificity for the enzyme since different catalytic components might be separated by a considerable margin in the free enzyme, minimizing the risk of a chance collision of the reactive group with both of them.

Although the lock-and key and induced-fit models can explain enzyme specificity, neither suggests any direct mechanism by which the catalyzed reaction may be driven forward. Substrate-binding often involves the expenditure of a considerable amount of energy and, although it serves a very useful purpose in bringing reaction and catalytic groups together, further energy must be supplied before the reaction can proceed.

Haldane, in 1930, pointed out that if the binding energy was used to distort the substrate in such a way as to facilitate the subsequent reaction, then less energy would be required for the reaction to take place. This concept was developed further by Pauling, in 1948. For example, there is a structure of the active site which is almost complementary to

that of a substrate, but not exactly so. If the structure of active site is rigid, the substrate must be distorted slightly in order to bind to the enzyme. This distortion might result in the stretching, and thus weakening, of a bond which is subsequently to be cleaved, thus assisting the forward reaction.

An alternative and more likely mechanism for driving the reaction forward is **transition-state stabilization**. This assumes that the substrate is bound in an undistorted form, but the enzyme-substrate complex possesses various unfavorable interactions. These tend to distort the substrate in such way as to favour the following reaction sequence: enzyme-substrate complex—transition-state—products. As the reaction proceeds, the unfavorable interactions diminish, and are absent from the transition-state. For a substance to be the substrate for an enzyme, the following two conditions are essential: firstly, substrate must have a susceptible chemical bond that can be attacked by the enzyme; secondly, is usually has some other structural features required for its binding to the enzyme active site, presumably to position the substrate molecule in the proper geometrical form so that the susceptible bond can be attacked by the enzyme.

In general, irrespective of the mechanism of an enzyme-catalyzed reaction, the major factor governing specificity is the stability of the enzyme-bound transition-state which exists during the conversion of enzyme-bound substrate to products. A potential substrate which can form a relatively stable transition-state when bound to the enzyme will be converted to products at an appreciable rate.

Chapter 2

Enzyme Kinetics

2.1 Factors Affecting Enzyme Activity

Knowledge of basic enzyme kinetic theory is important in enzyme analysis in order both to understand the basic enzymatic mechanism and to select a method for enzyme analysis. Several factors affect the rate at which enzymatic reactions precede - **temperature, pH, substrate concentration, and the presence of any inhibitors or activators.**

Like most chemical reactions, the rate of an enzyme-catalyzed reaction increases as the temperature is raised. [21, 22] A ten degree centigrade rise in temperature will increase the activity of most enzymes by 50 to 100%. Variations in reaction temperature as small as 1 or 2 degrees may introduce changes of 10 to 20% in the results. In the case of enzymatic reactions, this is complicated by the fact that many enzymes are adversely affected by high temperatures. The reaction rate increases with temperature to a maximum level, then abruptly declines with further increase of temperature. Because most animal enzymes rapidly become denatured at temperatures above 40 °C, most enzyme determinations are carried out somewhat below that temperature (**Figure 4**).

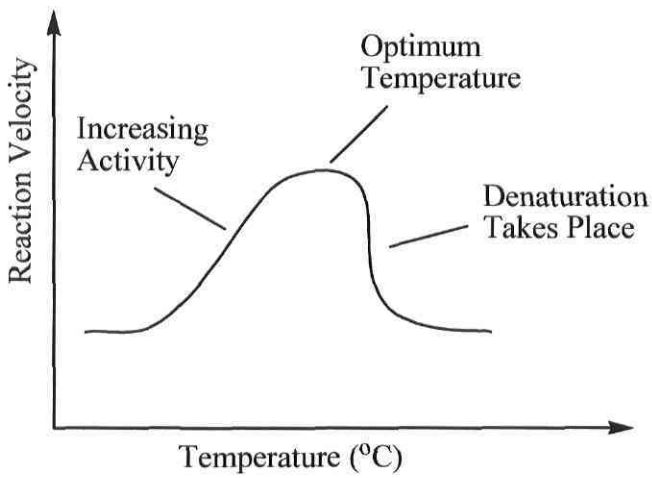

Figure 4. Effect of temperature on reaction rate.

Enzymes are affected by changes in pH. The most favorable pH value - the point where the enzyme is most active - is known as the optimum pH. Extremely high or low pH values generally result in complete loss of activity for most enzymes. pH is also a factor in the stability of enzymes. As with activity, for each enzyme there is also a region of pH optimal stability. Changes in the pH or acidity of the environment can take place that would alter or totally inhibit the enzyme from catalyzing a reaction. This change in the pH will affect the polar and non-polar intramolecular attractive and repulsive forces and alter the shape of the enzyme and the active site as well to the point where the substrate molecule could no longer fit, and the chemical change would be inhibited from taking place as efficiently or not at all. In an acid solution any basic groups such as the nitrogen groups in the protein would be protonated. If the environment was too basic the acid groups would be deprotonated. This would alter the electrical attractions between polar groups. Every enzyme has an optimum pH range outside of which the enzyme is inhibited. Correcting pH or temperature imbalances will usually allow the enzyme to resume its original shape or conformation. Some substances when added to the system will irreversibly break bonds disrupting the primary structure so that the enzyme is inhibited permanently. The enzyme is said to be irreversibly denatured. Many toxic substances will break covalent bonds and cause the unraveling of the protein enzyme. Other toxic substances will precipitate enzymes effectively removing them from the solution thus preventing them from catalyzing the reaction. This is also called denaturation.

Enzymes behave like any other catalysts in forming with the reactants a transition-state of lower free energy than that which would be found in the uncatalyzed reaction. For a single-substrate reaction, the enzyme initially binds the substrate at the specific binding-site to form an enzyme-substrate complex *ES* which undergoes a further reaction to breakdown to enzyme and product *P*:

$$E + S \xrightarrow{k_1} ES \xrightarrow{k_2} E + P$$

The overall rate of reaction (the rate of formation of P) must be limited by the amount of enzyme available and by the rate of breakdown of the enzyme-substrate complex. If the substrate concentration is sufficiently high it will "saturate" the enzyme and, therefore, force an immediate reaction with each available enzyme molecule to form an enzyme-substrate complex. Under these conditions there will be no free enzyme present and the concentration of enzyme-substrate complex $[ES]$ will be the total enzyme concentration present $[E_0]$, making the overall rate of reaction $k_2[E_0]$. This is independent of substrate concentration and so can not be increased by using still higher substrate concentrations. Therefore, it is the maximum initial velocity V_{max} possible at this enzyme concentration:

$$V_{max} = k_2[E_0].$$

Relatively small changes in activation energy can greatly alter the rate of reaction: an enzyme which reduces the activation energy from 100 kJ.mol^{-1} to 60 kJ.mol^{-1}, increases the reaction rate by about 10 million.

2.2 Michaelis-Menten Equation

In typical enzyme-catalyzed reactions, reactant and product concentrations are usually hundreds or thousands of times greater than the enzyme concentration. Consequently, each enzyme molecule catalyzes the conversion to product of many reactant molecules. The effect of substrate concentration on the initial rate of an enzyme-catalyzed reaction is a central concept in enzyme kinetics. When data are generated from experiments of this type and the results plotted as a graph of initial rate v_0 against substrate concentration $[S_0]$, many enzymes exhibit a rectangular hyperbolic curve (**Figure 5**).

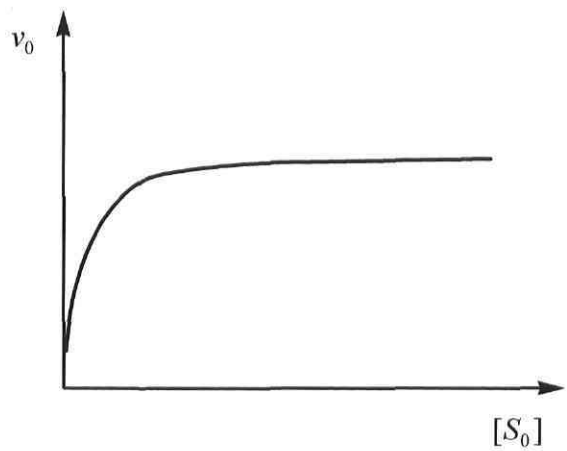

Figure 5. Graph of initial velocity against initial substrate concentration at constant total enzyme concentration for a single-substrate enzyme-catalyzed reaction.

Such a graph has the general equation

$$v_0 = \frac{V_{\max}[S_0]}{[S_0]+b}$$

where V_{max} is the maximum v_o at a particular total enzyme concentration and b is another constant.

Kinetic models to explain these findings were proposed by Henri (1903) and Michaelis and Menten (1913). The simplest general equation for a single-substrate enzyme-catalyzed reaction where there is just one substrate-binding site per enzyme is following:

$$E + S \underset{k_{-1}}{\overset{k_1}{\rightleftharpoons}} ES \xrightarrow{k_2} E + P$$

The terms k_1, k_{-1} and k_2 are rate constants for, respectively, the association of substrate and enzyme, the dissociation of unaltered substrate from the enzyme and the dissociation of product (= altered substrate) from the enzyme. The theoretical possibility of a reverse reaction with ES complex forming from E and P can be ignored because we are considering *initial* rates of reaction, i.e. when the enzyme is first provided with substrate, so there should not be any product available to combine with enzyme.

The Michalis-Menten assumption was that equilibrium between enzyme, substrate and enzyme-substrate complex was almost instantly set up and maintained, the breakdown of enzyme-substrate complex to products being too slow to disturb this equilibrium. Using this assumption, therefore:

$$k_1[E][S] = k_{-1}[ES]$$

$$\frac{[E][S]}{[ES]} = \frac{k_{-1}}{k_1} = K_s$$

where K_s is the dissociation constant of enzyme-substrate complex *ES*.

The total concentration of enzyme present $[E_0]$ must be the sum of the concentration of free enzyme $[E]$ and of the concentration of bound enzyme $[ES]$:

$$[E] = [E_0] - [ES]$$

$$\frac{([E_0]-[ES])[S]}{[ES]} = K_s,$$

$$[ES] = \frac{[E_0][S]}{[S]+K_s}.$$

The overall rate of the reaction v_0 is limited by the step ES → E + P, and this will depend on two factors - the rate of that step (i.e. k_2) and the concentration of enzyme that has substrate bound, i.e. $[ES]$. This can be written as:

$$v_0 = k_2[ES]$$

So we obtain:

$$v_0 = \frac{k_2[E_0][S]}{[S]+K_s}$$

When the substrate concentration is very high, the entire enzyme is present as the enzyme-substrate complex and the limiting initial velocity V_{max} is reached. Under these conditions:

$$V_{\max} = k_2[E_0],$$

$$v_0 = \frac{V_{\max}[S]}{[S]+K_s}.$$

The second assumption of Michaelis and Menten is that the substrate is usually present in much greater concentration than the enzyme. So if to make the assumption that the initial substrate concentration $[S_0]$ is very much greater than the initial concentration $[E_0]$, then the formation of the enzyme-substrate complex will result in an insignificant change in free substrate concentration.

Hence,

$$v_0 = \frac{V_{\max}[S_0]}{[S_0]+K_s}.$$

This is an equation of the form required to explain the experimental findings.

Briggs and Haldan (1925) modified the equation derived by Michaelis and Menten. They introduced a more generally valid assumption, that of the steady-state, i.e. *ES* complex is being formed and broken down at the same rate, so the overall [*ES*] is constant. The formation of *ES* will depend on the rate constant k_1 and the availability of enzyme and substrate, i.e. [*E*] and [*S*]. The breakdown of [*ES*] can occur in two ways, either the conversion of substrate to product or the non-reactive dissociation of substrate from the complex. In both instances the [*ES*] will be significant. Thus, using the steady-state assumption, we can write:

$$k_1[E][S] = k_{-1}[ES] + k_2[ES] = [ES](k_{-1} + k_2),$$

$$\frac{[E][S]}{[ES]} = \frac{k_{-1} + k_2}{k_1} = K_m$$

where K_m is another constant.

Substituting

$$[E] = [E_0] - [ES] \quad \text{as before:}$$

$$\frac{([E_0] - [ES])[S]}{[ES]} = K_m$$

from which

$$[ES] = \frac{[E_0][S]}{[S] + K_m}.$$

Again, since

$$v_0 = k_2[ES],$$

$$v_0 = \frac{k_2[E_0][S]}{[S] + K_m}$$

And since

$$V_{\max} = k_2[E_0],$$

$$v_0 = \frac{V_{\max}[S]}{[S] + K_m}.$$

Finally, since the substrate concentration is usually much greater than the enzyme concentration, $[S] \cong [S_0]$, so

$$v_0 = \frac{V_{\max}[S_0]}{[S_0] + K_m} \text{ at constant } [E_0].$$

This equation has retained the name **Michaelis-Menten equation** and K_m is the **Michaelis constant**. The equilibrium-assumption is a special case of the more general steady-state-assumption, occurring where $k_{-1} \gg k_2$.

A graph of v_0 against $[S_0]$ will have the form of rectangular hyperbola (**Figure 6**) consistent with experimental findings for many enzyme-catalyzed reactions.

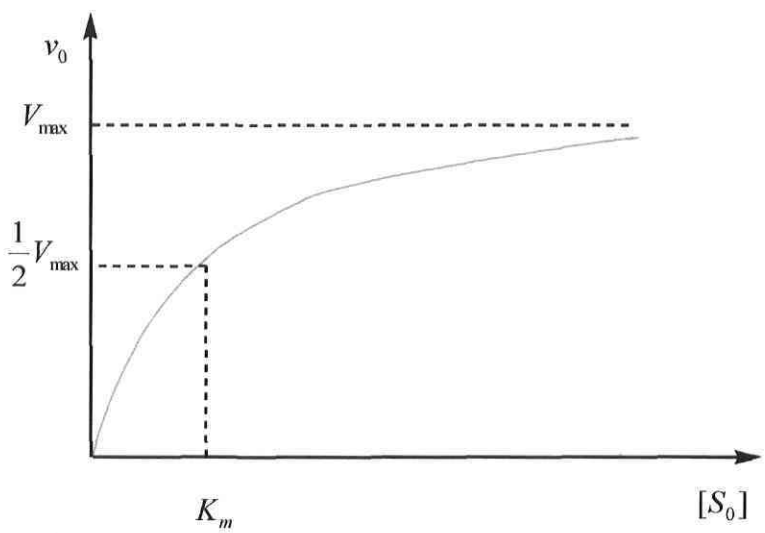

Figure 6. Graph of v_0 against $[S_0]$ at constant $[E_0]$ for a single-substrate enzyme-catalyzed reaction, from Michaelis-Menten equation.

K_m is an indicator of the affinity that an enzyme has for a given substrate, and hence the stability of the enzyme-substrate complex.

When

$$v_0 = \frac{V_{\max}}{2},$$

$$K_m = [S_0].$$

Therefore, K_m is the value of $[S_0]$ which gives an initial velocity equal to $V_{\max}/2$.

2.3 The Lineweaver-Burk equation

The graph of the Michaelis-Menten equation is not entirely satisfactory for the determination of $V_{\max}$ and K_m. After a series of experiments there are at least three consistent points of the plateau of the curve at different $[S_0]$ values, so an accurate value of $V_{\max}$, and hence of K_m cannot be obtained: the graph, being a curve, cannot be accurately extrapolated upwards from non-saturating values of $[S_0]$.

Lineweaver and Burk (1934) overcame this problem. They simply took the Michaelis-Menten equation

$$v_0 = \frac{V_{\max}[S_0]}{[S_0] + K_m}$$

and inverted it:

$$\frac{1}{v_0} = \frac{[S_0] + K_m}{V_{\max}[S_0]}$$

$$\frac{1}{v_0} = \frac{K_m}{V_{max}} \frac{1}{[S_0]} + \frac{1}{V_{max}}.$$

This is the **Lineweaver-Burk plot** for systems obeying the Michaelis-Menten equation.

The graph, being linear, can be extrapolated even if no experiment has been performed at a saturating substrate concentration, and from the extrapolated graph the values of K_m and V_{max} can be determined (**Figure 7**).

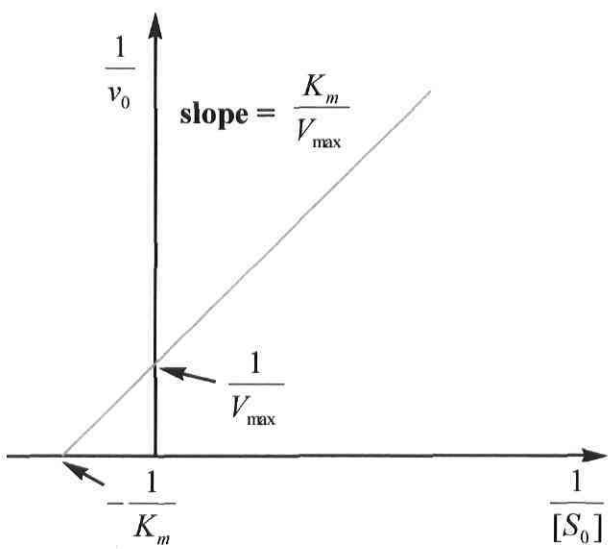

Figure 7. The Lineweaver-Burk plot.

Chapter 3

Enzymes Involved in Tyrosine Catabolic Pathway: Description and Potential Inhibitors

As mentioned above, the deficiency of one of the enzymes involved in the tyrosine catabolic pathway leads to the different hereditary diseases. Thus, the determination of crystal structure and the study of the mechanism of action of these enzymes have become in the focus of considerable research interest. This knowledge may help to better understand the causes of disease origin and be very useful to develop new potential inhibitors.

3.1 *p*-Hydroxyphenylpyruvate dioxygenase

2-(2-nitro-4-trifluoromethylbenzoyl)-1,3-cyclohexanedione (NTBC) administrated as Nitisinone (Swedish Orphan Int. AB) is the only known medicament which inhibits *p-hydroxyphenylpyruvate dioxygenase* (*p*-HPPD), the second enzyme in the tyrosine catabolic pathway.

p-HPPD (EC 1.13.11.27) is an important enzyme in tyrosine catabolism of most organisms. This is a non-heme Fe (II)-dependent enzyme. It catalyzes the conversion of *p*-hydroxyphenylpyruvic acid (*p*-HPPA) to homogentisic acid, HGA (2,5-dihydroxy-phenylacetic acid) and carbon dioxide (**Scheme 1**):

Scheme 1

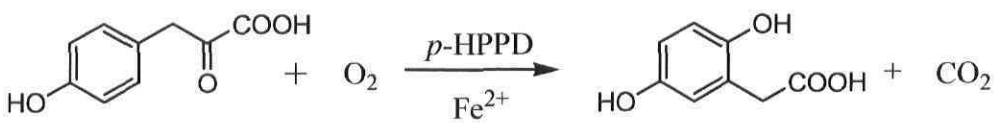

p-HPPD is found in the liver and kidney of mammals and has been isolated from bacteria. This enzyme belongs to the α-keto acid-dependent group of oxygenase.[23] All

studied mammalian *p*-HPPDs behave as homodimers of 43-49 kD subunits. Plant *p*-HPPDs resemble the mammalian enzyme in that it behaves as a homodimer with 48 kD subunits. All *p*-HPPD enzymes purified and studied so far contain Fe^{2+} as an essential cofactor (**Figure 8 a**). Consistent with amino acid sequence comparisons the active site structures reveal that two histidines and one acid residue are liganded to the iron in the active site of both proteins (**Figure 8 b**). [24]

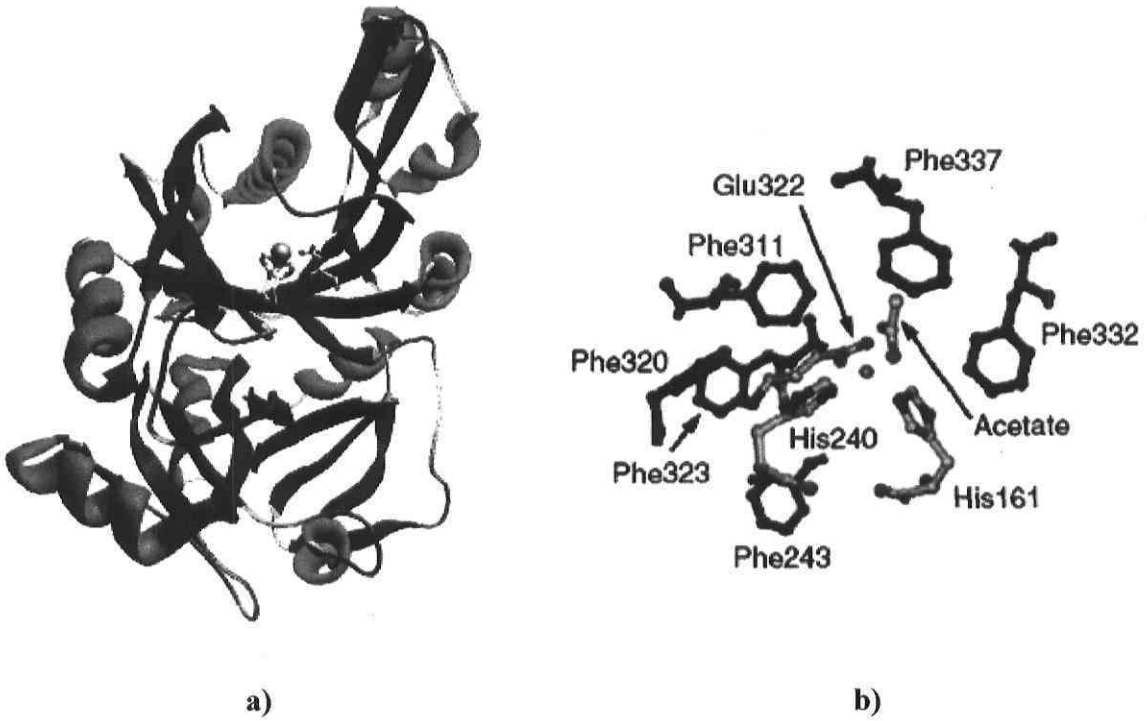

Figure 8. a) The crystal structure of *p*-HPPD. Helices are colored green; β-sheets are colored blue; a Fe^{2+} is colored grey. **b)** The active site of *p*-HPPD. Iron ion is represented by lilac sphere; two histidines and one acid residue are liganded to the iron in the active site.

The herbicidal activity of certain 2-benzoylcyclohexane-1,3-diones, referred to as triketones, was discovered in 1982 by Zeneca Agrochemical Products.[25] Members of the triketone family had been reported as naturally occurring compounds in plant oils of

Australian plants. From the knowledge of the herbicidal action of triketones emerged an initial observation that few plants grew under the Australian bottle-brush plant, *Calistemon* spp., and that the natural product leptospermone produced bleaching symptoms in plants. Subsequently the triketone group was extended to include herbicidal compounds incorporating a 1,3-cyclohexanedione ring. These compounds are broad-spectrum, bleaching herbicides. An early compound in this series was NTBC. The finding that NTBC causes elevated tyrosine levels in experimental animals led to the discovery of *p*-HPPD as the molecular target site of triketone herbicides.

It was shown then by Zeneca, in collaboration with the group of professor Sven Lindstedt[17] that NTBC caused highly specific inhibition of human and rat *p*-HPPD. The Swedish group, which was working on tyrosinemia type I recognized the potential of NTBC treatment. Detailed enzyme kinetic studies with rat liver cytosol showed that NTBC is not irreversible bound to the enzyme; the enzyme-inhibitor complex will dissociate with an estimated half-life *in vitro* at 25 °C of 63 hours. Thus, the interaction of NTBC with *p*-HPPD is characterized by a rapid inactivation step to form an enzyme-inhibitor complex that can dissociate slowly with recovery of enzyme activity. The kinetic results suggest that the triketones bind to the same part of the active site as the substrate.

There are two groups of the potential inhibitors of *p*-HPPD. The first one possesses a β-diketone moiety, which mimics the α-keto acid group of the substrate, *p-hydroxyphenylpyruvic acid* (*p*-HPPA) (**Table 2**).[26] Inhibition kinetics studies, binding of ^{14}C DKN (diketonitrile of isoxaflutole, the first known herbicidical compound possessing a β-diketone moiety) confirm that all these inhibitors compete with the substrate for the binding of the essential iron on the active site of the enzyme, and exert a tight binding inhibition, competitive with the substrate, *p*-HPPA. Thus, potent inhibitors of this kind must possess a tricarbonyl methane structure and one of the three carbonyl groups must be a substituted benzoyl group; the compounds must be able to enolise so that the enolate is capable of inhibiting *p*-HPPD enzyme by competitive combination with Fe^{2+}- the reaction center of *p*-HPPD enzyme.

Substrate	Herbicides
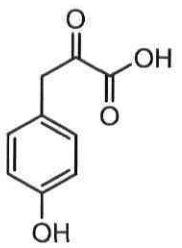 **p-Hydroxyphenylpyruvic acid** **p-HPPA**	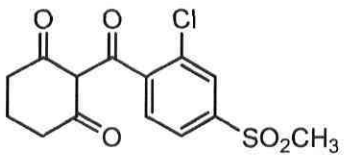 **Sulcotrione** 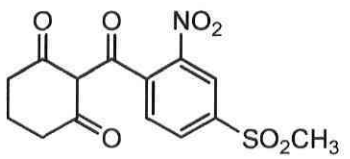 **Mesotrione** 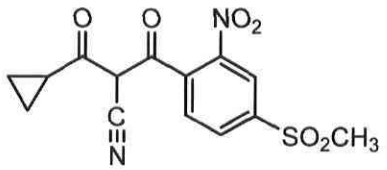 **Diketonitrile (DKN)**

Table 2. Chemical structure of herbicidal ligands of *p*-HPPD.
All the ligands share β-diketone moiety, which mimics the α-keto-acid chain of the substrate, *p*-HPPA.

The other group of *p*-HPPD potential inhibitors belongs to the non-triketone type. It has been shown that various enol ethers of allyloximes are more effective and selective herbicides than cyclohexanedione class herbicides.[27]

The group of scientifics from Tunghai Christian University has developed a new class of potent, low molecular weight, 3-cyclopropanecarbonyloxy-2-cyclohexen-1-one type of *p*-HPPD inhibitors (**Table 3**).[28] The compounds represented in this table have a very good inhibitor activity. Their IC_{50} are comparable to that of NTBC (IC_{50}=40 nM).

Table 3. Inhibition constants for non-triketone type potential inhibitors of *p*-HPPD.

Compound	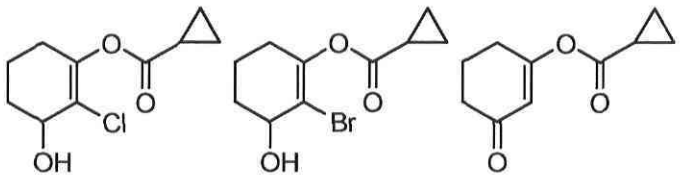		
IC_{50} (nM)	**15**	**28**	**30**

The investigation of structure-activity relationship (SAR) for this class of *p*-HPPD inhibitors is depicted in **Figure 9**. The two carbonyl groups as well as the cyclopropyl group of 3-cyclopropane-carbonyloxy-2-cyclohexen-1-one are required for potent *p*-HPPD. Substitution at the 2-position of ring system (R_1) has a significant effect on inhibitor potency, while the 5-position (R_2) can undergo substantial variations and retain inhibitor potency.

Thus, the derivatives of 3-cyclopropane-carbonyloxy-2-cyclohexen-1-one have the potential to serve as new therapeutic agents to treat the tyrosinemia type I.

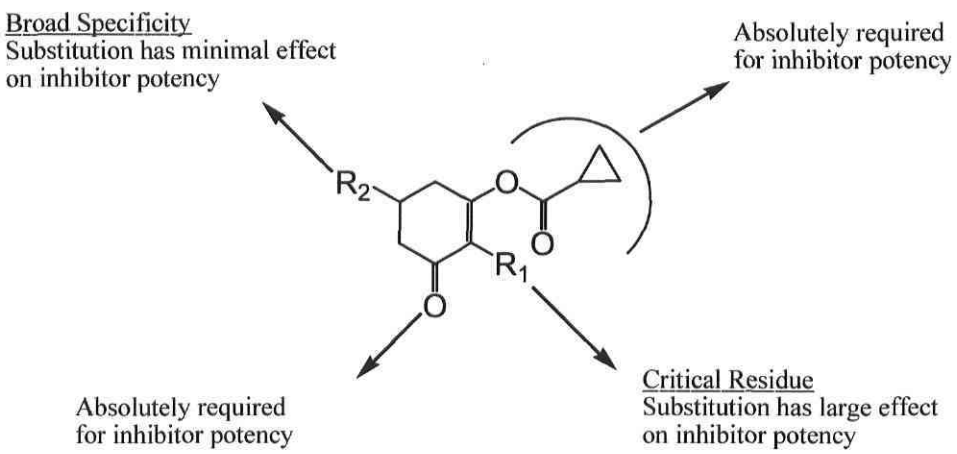

Figure 9. General SAR for 3-cyclopropanecarbonyloxy-2-cyclohexen-1-one inhibitors.

3.2 Fumarylacetoacetate hydrolase

Fumarylacetoacetate hydrolase (FAH) catalyzes the hydrolytic cleavage of carbon-carbon bond in fumarylacetoacetic acid to yield fumaric acid and acetoacetic acid as the final products of tyrosine degradation (**Scheme 2**).[29] This unusual reaction is an essential human metabolic function, because the loss of FAH activity causes the fatal metabolic disease hereditary tyrosinemia type I.

Scheme 2

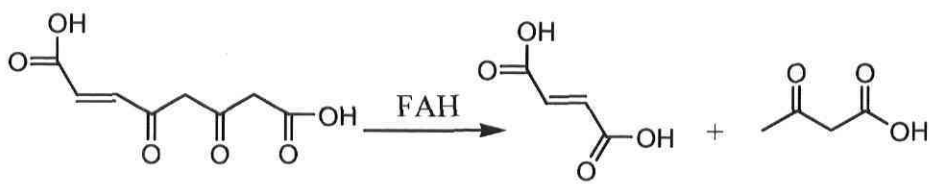

FAH (EC 3.7.1.2) is a homodimer of 46 kDa subunits that catalyzes the hydrolytic cleavage of carbon-carbon bonds in a variety of diketo acid substrates. The FAH structure consists of a 120-residue N-terminal domain of unknown function and a 300-residue C-terminal domain defined by a novel β-sandwich roll structure that forms an active site in close proximity to the dimer interface.

The FAH active site occurs in a solvent-filled cavity that is complementary in shape and charge to the fumarylacetoacetate substrate. The base of active site is formed by a metal ion coordinated by four side-chain carboxyl groups at the edge of the β-roll, whereas the sides are formed by helices and turns located above the β-rolls. Ca^{2+} is octahedral coordinated by carboxyl from Asp 126, Glu 199, Glu 201, Asp 233, an acetate molecule and water bound to the side chain oxygen of Thr350 (**Figure 10**).

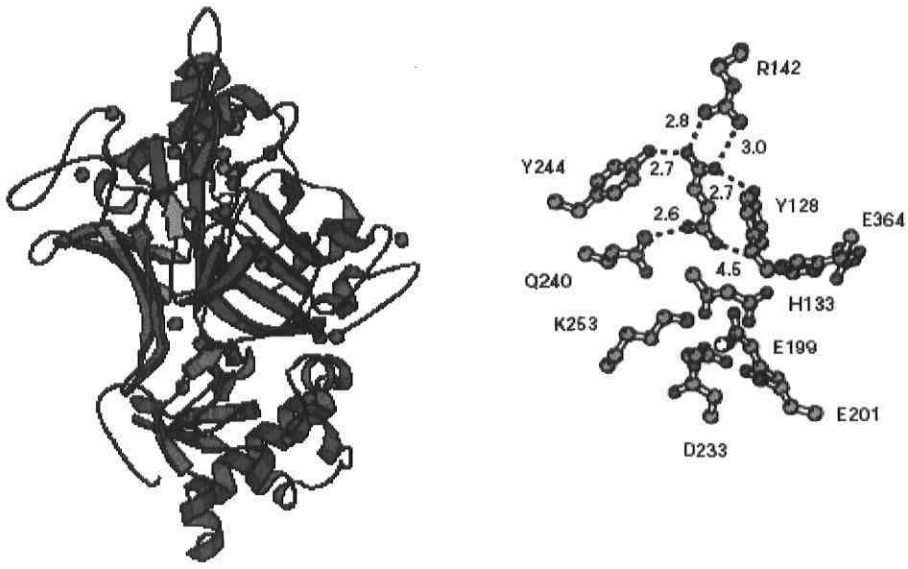

a) b)

Figure 10. a) The crystal structure of FHA. The N-terminal domain is located at the bottom of the figure. The mixed β-sandwich roll structure is centrally located. Helices are colored red; β-strands are colored in shades of blue corresponding to the β-sheet they form; a calcium ion is colored yellow. **b)** The active site of FHA. Carbon, nitrogen, oxygen and calcium are respectively colored orange, blue, red and yellow. Numbers are given for the interatomic distance (in Å) indicated by dashed lines.

It is known that molecules containing phosphorus are effective inhibitors of enzymes-catalyzed hydrolytic reactions. Substrate analogues containing phosphonate, phosphonoamidate, and phosphinate groups have been used as effective noncovalent inhibitors of aspartylproteases and metalloproteases.[30]

As an effective inhibitor of a carbon-carbon hydrolysis, 4-(hydroxymethyl-phosphinoyl)-3-oxo-butanoic acid (HMPOBA) represents the first example of phosphorus-based analog targeting this class of enzymes (**Figure 11**).[31]

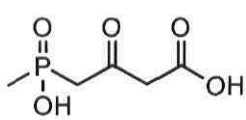

Figure 11. HMPOBA, noncovalent competitive inhibitor of FAH.

This is a noncovalent competitive inhibitor of FAH with a K_i, of 85μM. The kinetic studies have indicated that the tetrahedral geometry associated with the phosphorus groups in these types of inhibitors closely approximates both geometric and electronic aspects of the transition state. Thus, the effectiveness of these compounds as inhibitors is presumably associated with similarities to the high energy reaction intermediates stabilized during catalysis. These results provide a context for future structure-based design of FAH inhibitors and the additional insight into the mechanism by which FAH catalyzes the hydrolysis of carbon-carbon bond.

3.3 Homogentisate dioxygenase

Homogentisate dioxygenase (HGO) (E.C.1.13.11.5) catalyzes the crucial aromatic ring opening reaction, utilizing nonheme Fe^{2+} to incorporate both atoms of molecular oxygen into homogentisate (2,5-dihydroxyphenylacetate).[32] The HGO belongs to the catecholic extradiol dioxygenase family. It utilizes Fe^{2+} to cleave a bond located adjacent to only one hydroxyl group (**Scheme 3**).

Scheme 3

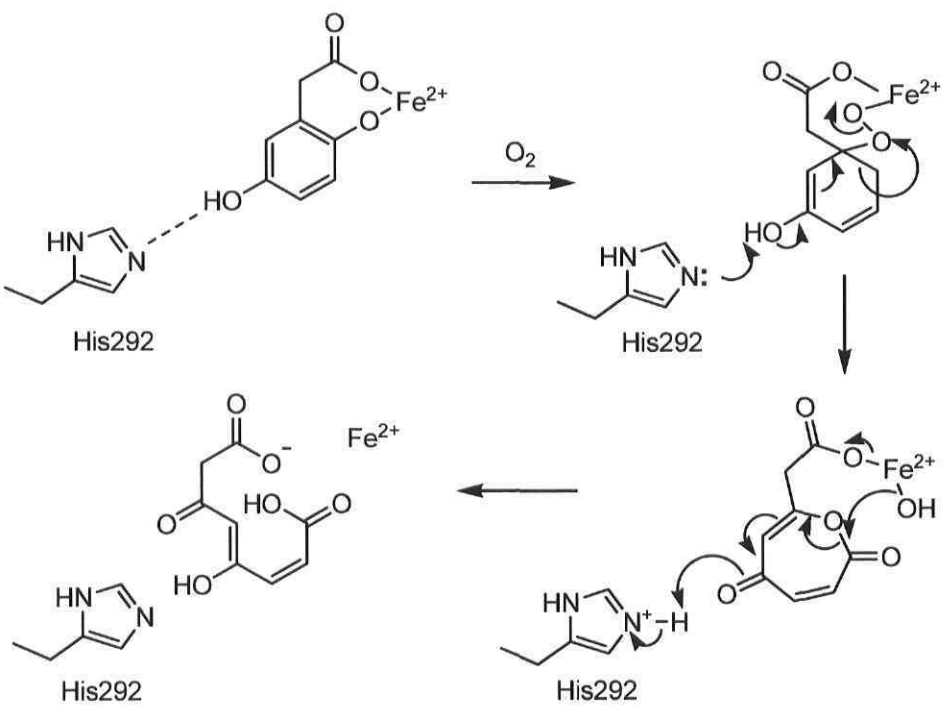

Human HGO is a hexameric enzyme (α_6) with a subunit molecular mass of approximately 50 kDa. A monomer contains five antiparallel β-sheets and one mixed β-sheet. The structure can be described as 280-residue N-terminal and 140-residue C-terminal domains. The central feature of the HGO structure is a jelly roll of β-strands in the N-terminal domain, which forms part of a β-sandwich between a nine-stranded antiparallel β-sheet and a seven-stranded mixed β-sheet.

The active site of HGO is formed by the seven-stranded C-terminal β-sheet, antiparallel section of polypeptide between Pro 320 and Lys 327 and between Met 368 and Lys 385, and loop between Phe 282 and Thr 299. A single iron ion is coordinated by the side chains of His 361, Glu 367 and His 397 located in the C-terminal domain near the interface between subunits in the HGO trimer. This facial triad is found in many mononuclear iron enzymes, including extradiol dioxygenases. The structure of HGO and it active site are represented in **Figure 12**.

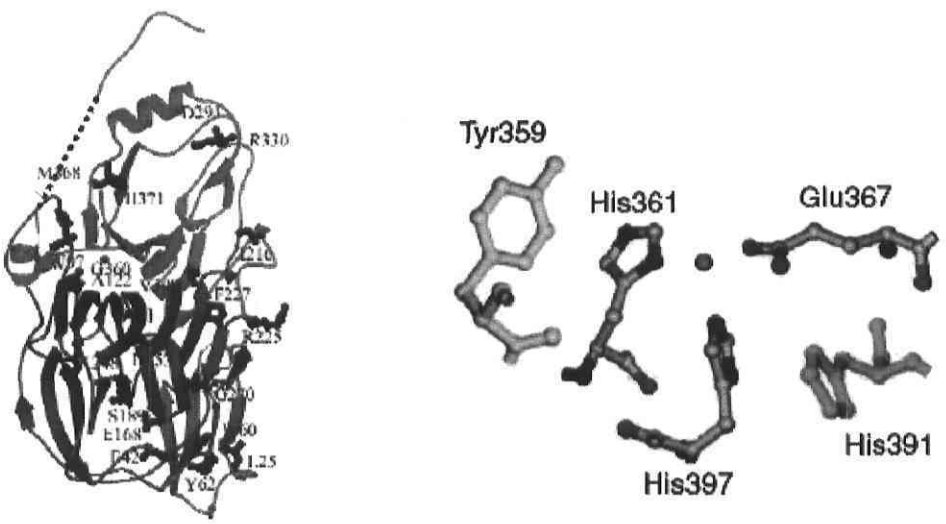

Figure 12. a) The crystal structure of HGO. The central β-sandwich is colored in dark blue, the C-terminal active site domain in green and the strands of the intersubunit β-sheet in light blue. **b)** The active site of HGO. A single iron ion, which is represented by lilac sphere, is coordinated by the side chains of His 361, Glu 367 and His 397 located in the C-terminal domain near the interface between subunits in the HGO trimer.

The homogentisate dioxygenase has been an enzyme of considerable interest since 1902, when Garrod demonstrated that AKU was inherited as a recessive Mendelian trait. AKU was used as the prototypic example to develop the fundamental concept of "inborn error of metabolism", a precedent for the "one gene one enzyme" concept of Beadle and Tatum. Moreover, it has been shown by Fernández-Cañón and Peñalva that the treatment of tyrosinemia type I with inhibition of HGO is more effective and less toxic than the treatment with NTBC.[33] In fact, the metabolite accumulating in the body as a result of inhibition of HGO is the homogentisic acid (HGA). The human is able to accumulate HGA about 1600 g per day without particular problems for the health.[2] Then, HGA can be taken out in urine in the form of the black pigment or can accumulate in the different tissues of the human. These observations have served as incitement to develop the potential inhibitors of HGO.

Extradiol-type dioxygenases can be inhibited or inactivated by halogenated substrate analogues. Thus, DHBD (2,3-dihydroxybiphenyl 2,3-dioxygenase) and C23O (catechol 2,3-dioxygenase) are reversibly inhibited by 3-Cl catehol in a mechanism that involves oxidation of the Fe^{2+} in active site.[34] The first halogenated analogue of HGA, 3-Cl-homogentisic acid (3-Cl HGA), has been synthesized in our laboratory by Geneviève Gingras. The group of professor Lindsay D. Eltis from University of British Columbia has investigated the steady-state kinetics and inhibition of human HGO by 3-Cl HGA. These results are represented in **Table 4**.[35]

Substrate	k_{cat}^{app} (s^{-1})	k_{A}^{app} ($x10^{6}M^{-1}s^{-1}$)	Partition ratio
HGA	56.0	2.51	13 700
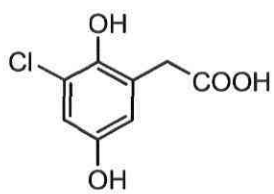 3-Cl-HGA	0.53	0.0241	79

Table 4. Apparent steady-state kinetic parameters of human HGO for different substrates.

We can see that the apparent specificity of HGO for HGA was 104 times higher than for 3-Cl HGA. However, the k_{cat}^{app} value is 100 times lower for 3-Cl HGA when compared with the value obtained with HGA. It means that the enzyme opens the benzene ring of 3-Cl HGA 100 times slower than the benzene ring of HGA. The partition ratio of HGO is much lower for 3-Cl HGA comparing to HGA that confirms as well the inhibitor properties of 3-Cl HGA for HGO.

Thus, the halogenated analogues of homogentisic acid represent very interesting targets for the synthesis of potential inhibitors of HGO. These compounds could play the crucial role in drug design to treat tyrosinemia type I.

Chapter 4

Synthesis of Potential Inhibitors of Human HGO

4.1. Choice of targets

As mentioned above, the first potential inhibitor of human HGO was synthesized by Geneviève Gingras in our laboratory. This is the substrate halogenated analogue, namely, 3-chlorohomogentisic acid (3-Cl HGA), which belongs to the irreversible suicidal type of inhibitors.

On the other hand, HGO does not appear to be as strongly inhibited by 3-Cl HGA as other extradiol-type dioxygenases are by chlorinated substrate analogues.[35] Thus, during further search of potential inhibitors of HGO three other halogenated analogs of HGA were synthesized in our laboratory (**Table** 5).

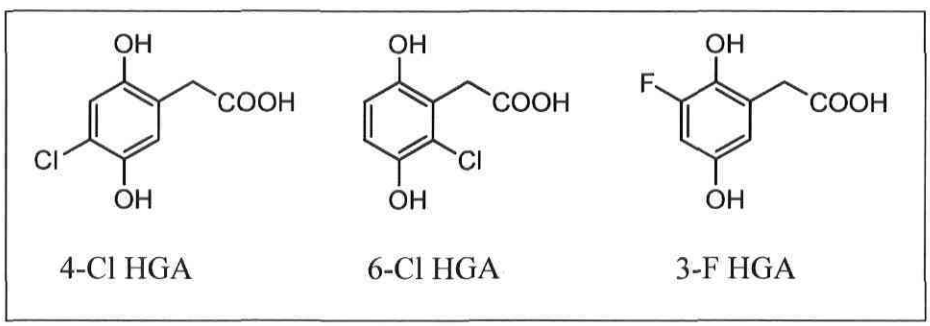

Table 5. The halogenated analogues of HGA as potential inhibitors of human HGO.

As can we see, 4-Cl HGA and 6-Cl HGA analogues differ from 3-Cl HGA just by the position of chlorine in benzene ring. This can entail the change in the inhibitor activity of human HGO in comparison with 3-Cl HGA. These compounds do not exist in literature; they have been synthesized for the first time in our laboratory.

One of the important applications of fluorinated organic compounds is in medicinal chemistry. In 1953, Fried published a pioneering work on the preparation of 9α-fluoro-hydrocortisone acetate. Utilization of fluorination as a tool to enhance biological activity

and to improve the versatility of a biologically active substance was thus clearly demonstrated.[36] Fluorine has a small van der Waals radius of 1.35 Å, close to that of hydrogen (1.20 Å). The C-F bond length, 1.38 Å, is comparable to that C-H, 1.10 Å, and C-O bond lengths, 1.43 Å. This means that the selective substitution of hydrogen for fluorine will have little effect on the steric bulk of a molecule but can alter the reactivity and change the biological efficiency. Introduction of fluorine into biologically active molecules is a very powerful and versatile tool for the design of new drugs on the basis of the rational elucidation of molecular recognition processes.

Therefore, 3-F HGA analogue represents a very interesting target as an inhibitor of human HGO. This compound exists in literature as a product of enzymatic oxidation of 2-fluoro-HPP by *p*-HPPD.[37] but there is no data on the synthesis of this compound. So, 3-F HGA has also been synthesized for the first time in our laboratory.

The 4-Cl HGA has been synthesized by Xue-Jing Zheng and will not be described in this thesis.

4.2 Synthesis of 6-chloro-2,5-dihydroxyphenylacetic acid (6-Cl HGA)

As a starting material for this synthesis we have chosen methyl 2,5-dihydroxy-benzoate (**1**). This compound already contains the important elements, namely two hydroxyl groups in benzene ring and an ester group. Thus we need to incorporate the chlorine in desirable position of benzene ring and to modify the side chain.

The full synthesis of 6-Cl HGA is represented in **Scheme 4**.

Scheme 4

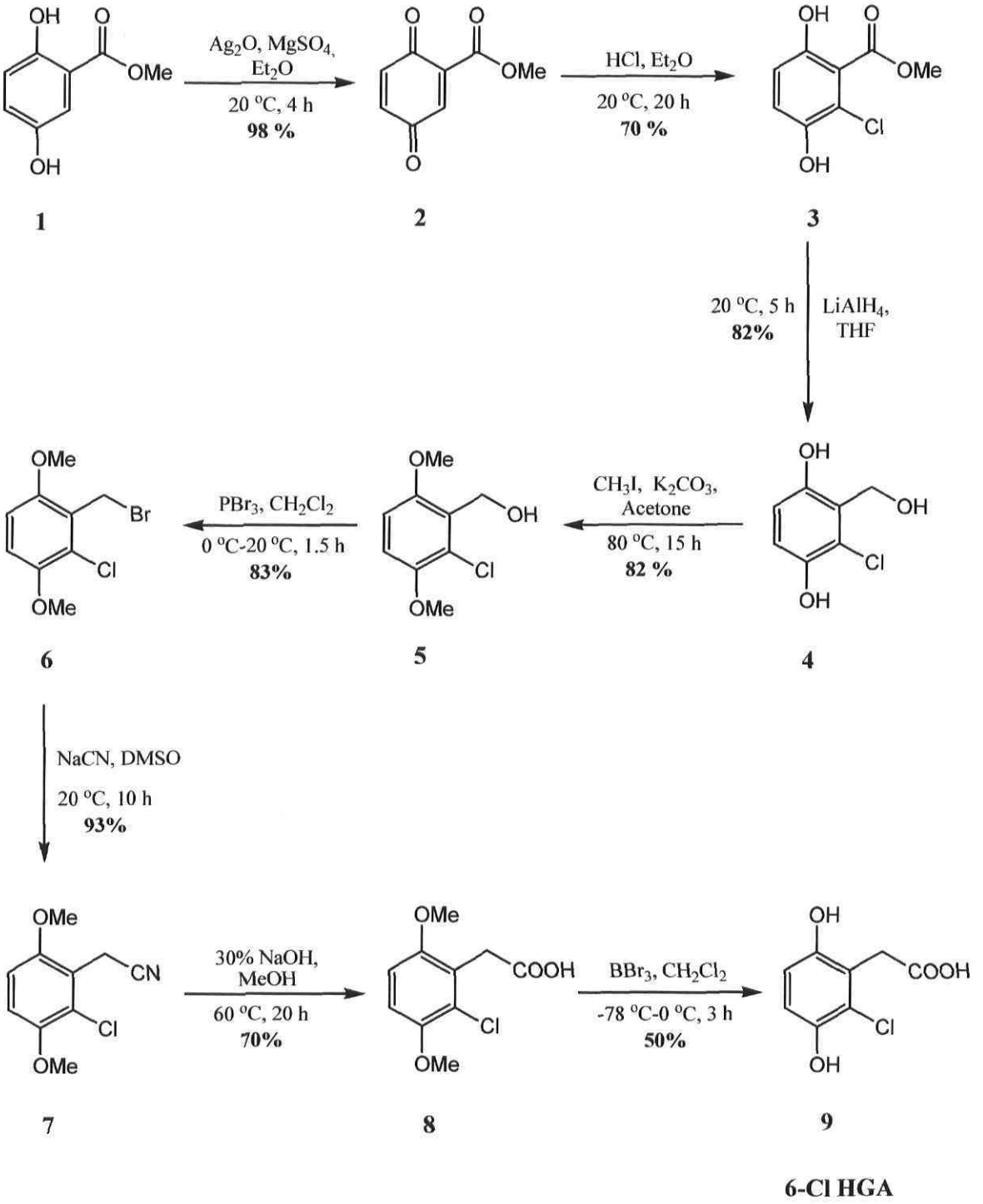
OH
O
OMe
OH
1
Ag2O, MgSO4,
Et2O
20 °C, 4 h
98 %
O
O
OMe
O
2
HCl, Et2O
20 °C, 20 h
70 %
OH
O
OMe
Cl
OH
3
20 °C, 5 h
82%
LiAlH4,
THF
OH
OH
Cl
OH
4
CH3I, K2CO3,
Acetone
80 °C, 15 h
82 %
OMe
OH
Cl
OMe
5
PBr3, CH2Cl2
0 °C-20 °C, 1.5 h
83%
OMe
Br
Cl
OMe
6
NaCN, DMSO
20 °C, 10 h
93%
OMe
CN
Cl
OMe
7
30% NaOH,
MeOH
60 °C, 20 h
70%
OMe
COOH
Cl
OMe
8
BBr3, CH2Cl2
-78 °C-0 °C, 3 h
50%
OH
COOH
Cl
OH
9
6-Cl HGA

The first step of the synthesis is oxidation of methyl 2,5-dihydroxybenzoate (**1**) to yield 2-(methoxycarbonyl)-1,4-benzoquinone (**2**) using silver oxide[38] (**Scheme 5**).

Scheme 5

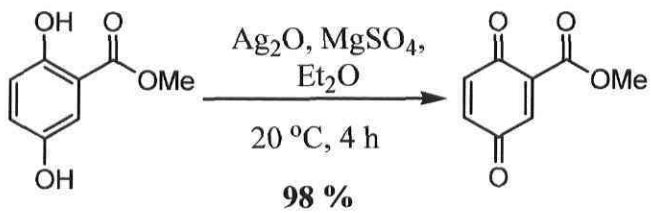

1 **2**

Methyl 2,5-dihydroxybenzoate (**1**) was placed with 3.0 equivalents of anhydrous magnesium sulfate as a moisture eliminator and 1.5 equivalents of silver oxide in ether solution. After 4 hours of reaction at 20 °C the product was separated from inorganic residue and evaporated to yield 2-(methoxycarbonyl)-1,4-benzoquinone (**2**). The yield of this reaction is 98%. This is a very convenient method of benzoquinone synthesis. The reaction proceeds under mild conditions with an excellent yield. The product does not require purification. However, it is important to notice that the yield of this procedure strongly depends on the freshness of silver oxide. The best of all is to prepare it directly before the reaction (for the method and details see the Experimental Section).

This is the redox reaction transfer generation. In this type of reactions there is one-electron transfer in generating the free radicals. The source of one-electron transfer is the metal ion, in our case Ag^{+}. The mechanism of this step is represented in **Scheme 6**. The forming anion is oxidized in two steps by silver ion loosing an electron at each stage. Two silver ions gain one electron apiece to become metallic silver. The intermediate in the oxidation is a radical anion known as semiquinone.

Scheme 6

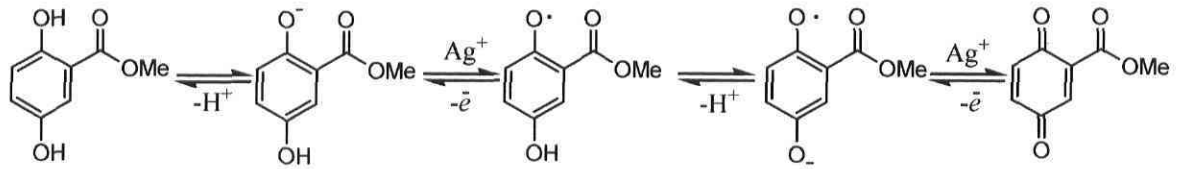

The second step of the synthesis of 6-Cl HGA is the crucial step because it is a question of chlorine incorporating in desirable position of the benzene ring (**Scheme 7**).

Scheme 7

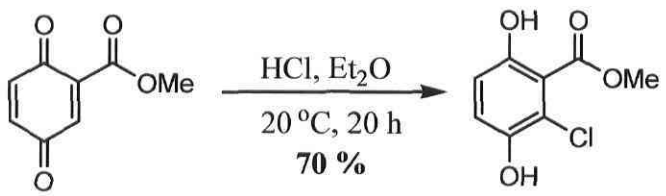

2 **3**

2-(Methoxycarbonyl)-1,4-benzoquinone (**2**) was placed with 3.5 equivalents of 2 M solution HCl in ether. After 20 hours of reaction at 20 °C the reaction mixture was purified on a silica gel column to yield methyl 6-chloro-2,5-dihydroxybenzoate (**3**). The yield of this reaction is 70%. Instead of HCl gas[39] we have used 2M solution of hydrogen chloride in ether as a source of Cl^-. This reagent is much more convenient because it is easy to handle and manipulate and the yield is much higher (70% versus 30% using HCl gas).

2-(Methoxycarbonyl)-1,4-benzoquinone (**2**) is an α,β-unsaturated ester. The addition of a nucleophilic carbon species to an α-β-unsaturated ester is called the Michael reaction. The anion of chlorine undergoes an 1,4-addition at the conjugated ester (**2**) forming the anion which has been then protonated (**Scheme 8**). After that the H-atom shift

takes place forming the aromatic system which is the driving force in this reaction and leading to the final product, methyl-6-chloro-2,5-dihydroxybenzoate (**3**).

Scheme 8

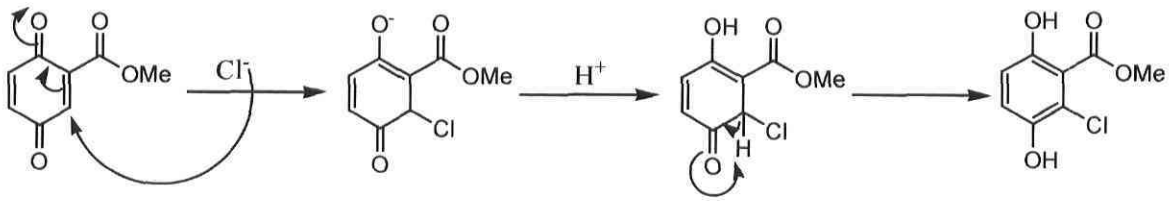

2 **3**

We can see that methyl 6-chloro-2,5-dihydroxybenzoate (**3**) already contains in the benzene ring all the substituents which we need for the final compound, 6-Cl HGA. All what we need now is to modify the side chain. But before this it is important to protect two phenolic groups. It is a very common operation in organic synthesis. We have decided to use the Williamson synthesis of ethers. For this, methyl 6-chloro-2,5-dihydroxybenzoate (**3**) was placed with 2.0 equivalents of K_2CO_3 and 3.0 equivalents of CH_3I in acetone. Unfortunately, after 24 hours of reaction at reflux the product has not formed. The probable explanation of this result may be following: the Williamson synthesis of ethers converts alcohols into ethers via S_N2 mechanism. Methyl 6-chloro-2,5-dihydroxybenzoate (**3**) contains two substitutes in adjacent positions to two hydroxyl groups which hinder the S_N2 attack of CH_3I and do not allow forming the protected product.

We have changed the plan of synthesis, namely, we have decided firstly to reduce the ester group using $LiAlH_4$ as a reduced reagent of reductor[40] (**Scheme 9**). In this reaction methyl 6-chloro-2,5-dihydroxybenzoate (**3**) was added to 2.0 equivalents of the solution of $LiAlH_4$ in tetrahydrofuran at 0 °C. Then, after 5 hours of reaction at 20 °C the product was separated from inorganic residue and subjected to column chromatography to get 6-chloro-2,5-dihydroxybenzyl alcohol (**4**) in 82% yield.

Scheme 9

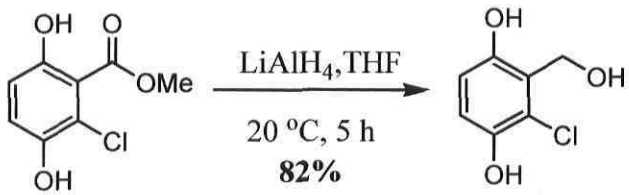

3 **4**

Using alternative reagent for this type of reduction, namely, DIBAL-H[41], is less effective because the reaction requires more time to finish and the yield is lower (70%).

Now we have tried again to protect selectively two phenolic groups (**Scheme 10**) using the Williamson synthesis of ethers. For this 6-chloro-2,5-dihydroxybenzyl alcohol (**4**) was placed with 2.0 equivalents of K_2CO_3 and 2.0 equivalents of CH_3I in acetone. The reaction lasted at reflux for 15 hours. After that the inorganic layer was filtered and the product was subjected to column chromatography to yield 6-chloro-2,5-dimethoxybenzyl alcohol (**5**). This time the reaction has proceeded with excellent yield (82%).

Scheme 10

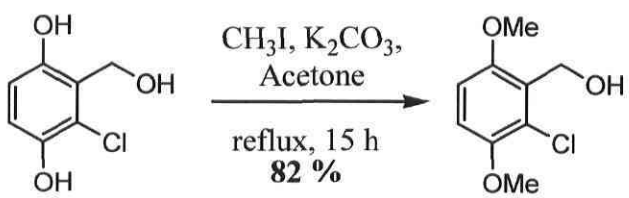

4 **5**

The next step of the synthesis of 6-Cl HGA is an activation of hydroxyl group of (**5**). It is a very common procedure in organic synthesis because the hydroxyl group is a poor leaving group. For this we have followed the procedure of transformation of 6-chloro-

2,5-dimethoxybenzyl alcohol (**5**) into 6-chloro-2,5-dimethoxybenzylmethane-sulfonate (**10**)[42] (**Scheme 11**).

Scheme 11

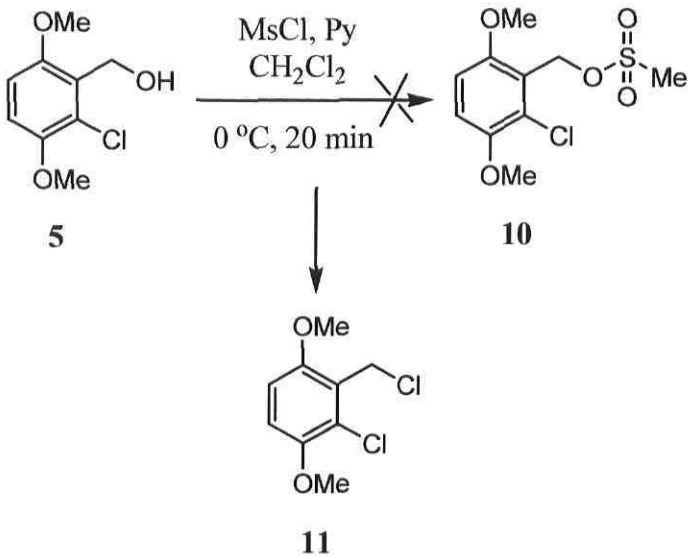

5 **10** **11**

However, the ^1H and ^{13}C spectral data of the product have shown us very interesting results. First of all, in the ^1H spectrum the peak corresponding to methyl in methanesulfonate group was absent whereas the singlet at δ 4.83 ppm was present which corresponds to the alkyl halide group in the side chain. The peak at δ 38.31 ppm in the ^{13}C spectrum also corresponds to the alkyl halide group. Thus, we have supposed that the product of reaction was chloromethyl-6-chloro-2,5-dimethoxybenzene (**11**) instead of expected 6-chloro-2,5-dimethoxybenzylmethanesulfonate (**10**). To confirm this supposition we have synthesized the compound (**11**). For this 6-chloro-2,5-dimethoxybenzyl alcohol (**5**) was placed with 1.0 equivalent of triphenylphosphine in CCl_4. After 24 hours of reaction at 40 °C the product was subjected to column chromatography. The ^1H and ^{13}C spectra data of purified compound were identical to those mentioned above.

We may presume that firstly formed 6-chloro-2,5-dimethoxybenzylmethane sulfonate (**10**) undergoes further transformation (**Scheme 12**). Methanesulfonate anion,

which is a very good leaving group, goes away. The benzyl cation formed in this process is very stable and then undergoes S_N1 attack of chloride anion forming the product (**11**).

Scheme 12

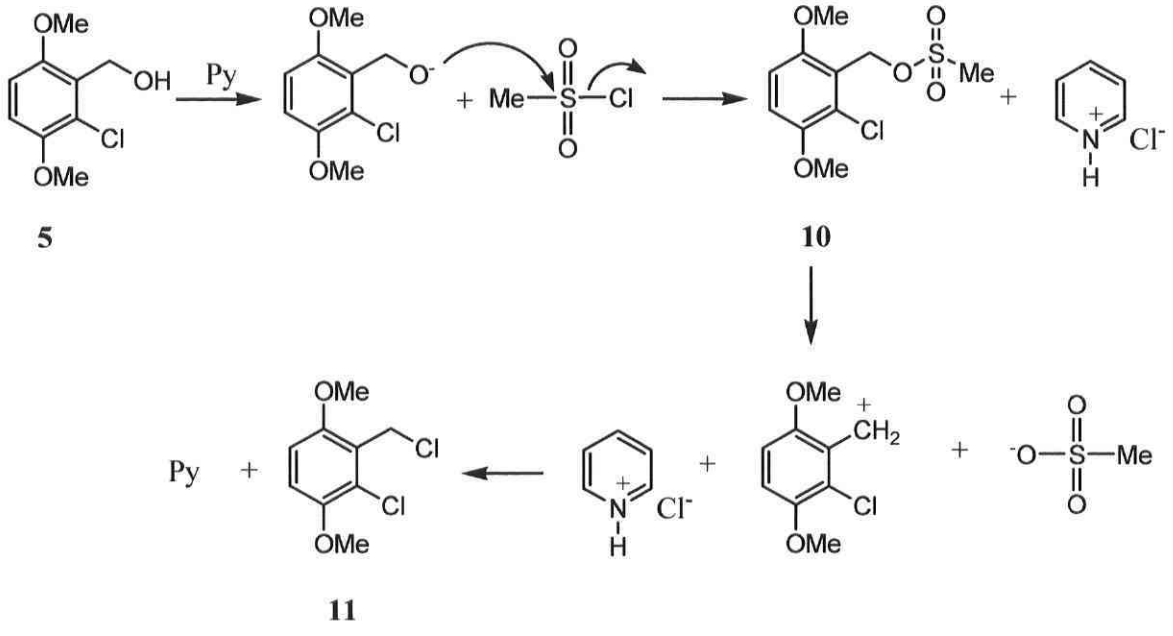

These results were very useful for us because they have us shown another possibility to continue the synthesis. It is a question of transformation of 6-chloro-2,5-dimethoxybenzyl alcohol (**5**) into corresponding alkyl halide **(Scheme 13)**. As a reagent we have chosen 1M solution of phosphorus tribromide in dichloromethane.[43]

Scheme 13

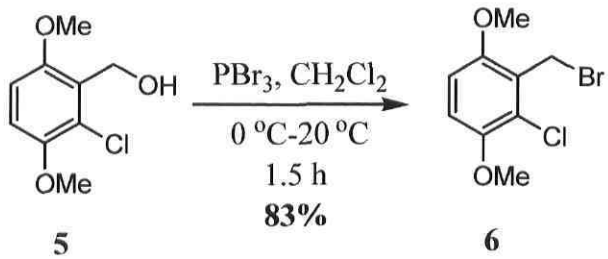

5 **6**

To a cooled (0 °C) solution of 6-chloro-2,5-dimethoxybenzyl alcohol (**5**) in dichloromethane was added 1.5 equivalents of 1M PBr_3 in CH_2Cl_2. After 1.5 hours of reaction at 20 °C the solvent was evaporated and the product was purified on a silica gel column to get the bromomethyl-6-chloro-2,5-dimethoxybenzene (**6**). This time the reaction proceeds smoothly with excellent yield (83%).

Now, there is the time to incorporate one more carbon atom by transformation of bromomethyl-6-chloro-2,5-dimethoxybenzene (**6**) into 6-chloro-2,5-dimethoxyphenyl-acetonitrile (**7**) (**Scheme 14**). This reaction smoothly proceeds via S_N2 substitution Br^- by CN^-.

Methylbromide-6-chloro-2,5-dimethoxybenzene (**6**) was placed with 1.5 equivalents of sodium cyanide in dimethylsulfoxide solution. After 10 hours of reaction at 20 °C 6-chloro-2, 5-dimethoxyphenylacetonitrile (**7**) was obtained in 93% yield after chromatography.

Scheme 14

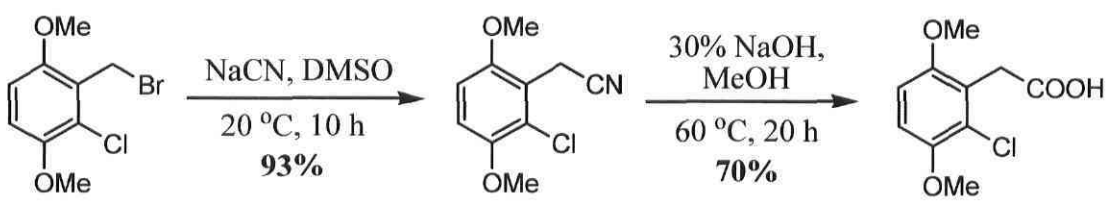

6 **7** **8**

6-Chloro-2,5-dimethoxyphenylacetic acid (**8**) was yielded by hydrolysis of (**7**) under basic conditions using 30% sodium hydroxide solution and methanol. This reaction lasts 20 hours at 60 °C and with 70% yield of product after chromatography. Hydrolysis of nitrile can be accomplished both the acidic and basic conditions. In our case we have chosen the basic condition to avoid the deprotection of phenol groups and the formation of corresponding lactone.

The final step of the synthesis is deprotection of two hydroxyl groups. Usually, this deprotection is carried out under drastic acidic conditions (for example HBr at reflux).[44] However, in our case using these conditions may lead to undesirable lactonisation of deprotected carboxylic acid. Geneviève Gingras tried to use different reagents[45] to avoid this problem and to reach a good yield during the synthesis of 3-Cl HGA. The best reagent was 1 M solution of boron tribromide in dichloromethane. We have also followed the protocol of Geneviève Gingras: we have used this reagent and have run the reaction at 20 °C for 10 hours. But the yield of final compound (**9**) was just 35%. Moreover, the content of lactone (control by means of TLC chromatography) was quite considerable. So, we have changed this protocol (**Scheme 15**).

Scheme 15

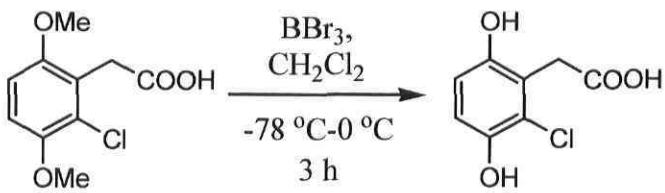

8 **9**

6-Chloro-2,5-dimethoxyphenylacetic acid (**8**) was placed with 2.5 equivalents of 1M BBr_3 in dichloromethane at -78 °C. After 1 hour the temperature was increased to 0 °C and after two hours in the reaction some cold water was added. This procedure is very important because it allows separating the carboxylic acid from the small quantity of

lactone which still forms during the reaction. Indeed, the carboxylic acid dissolves in water whereas the formed lactone stays in dichloromethane layer. Then the purification of product on a silica gel column provided 6-chloro-2,5-dihydroxyphenylacetic acid (**9**) in 50% yield.

There are several causes to explain this moderate yield. The first is the lactone formation during the reaction. The second is the partial decomposition of the product (**9**) on the silica gel column when in use of purification. This is very polar compound which makes difficult the fast purification.

Thus, the synthesis of 6-chloro-2,5-dihydroxyphenylacetic acid (6-Cl HGA) (**9**) has been accomplished in 8 steps and 12.5% overall yield.

4.3 Synthesis of 3-fluoro-2,5-dihydroxyphenylacetic acid (3-F HGA)

We have chosen 2-fluoro-4-methoxyphenol (**12**) as a started material. This compound already contains the fluorine atom in the desirable position of benzene ring. Subsequent selective ortho-hydroxymethylation of (**12**) allows synthesizing an intermediate (**13**) which contains in benzene ring the same substituents as that the final compound. The following modification of the side chain of (**13**) leads to 3-fluoro-2,5-dihydroxyphenylacetic acid (**18**) (**Scheme 16**).

Scheme 16

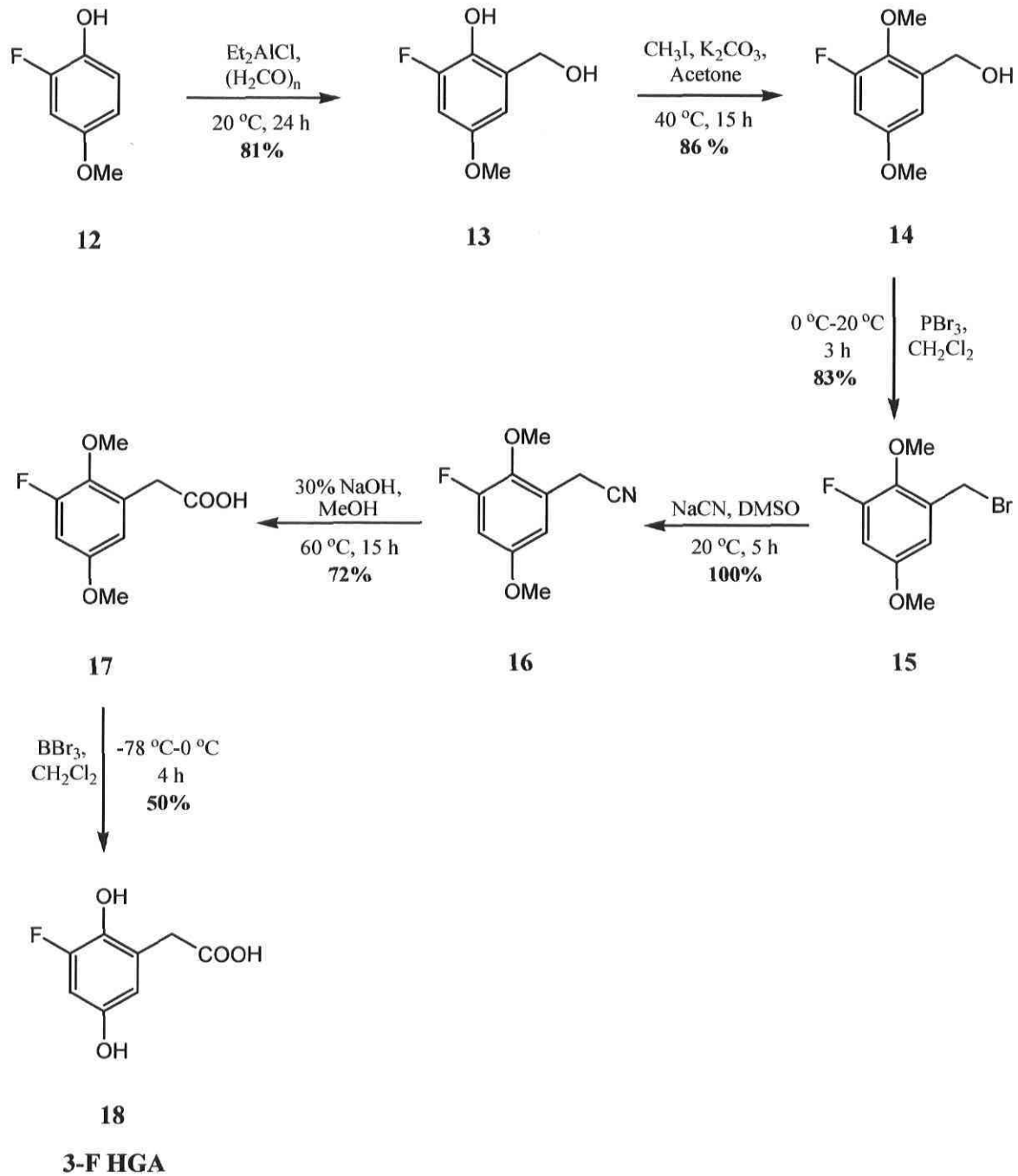
OH
F
OMe
12
Et2AlCl,
(H2CO)n
20 °C, 24 h
81%
OH
F
OH
OMe
13
CH3I, K2CO3,
Acetone
40 °C, 15 h
86 %
OMe
F
OH
OMe
14
0 °C-20 °C
3 h
83%
PBr3,
CH2Cl2
OMe
F
Br
OMe
15
NaCN, DMSO
20 °C, 5 h
100%
OMe
F
CN
OMe
16
30% NaOH,
MeOH
60 °C, 15 h
72%
OMe
F
COOH
OMe
17
BBr3,
CH2Cl2
-78 °C-0 °C
4 h
50%
OH
F
COOH
OH
18
3-F HGA

The first step of this synthesis is a very interesting. It is a questing of ortho-specific hydroxyalkylation of 2-fluoro-4-methoxyphenol (**12**). We have tried to synthesize the 3-fluoro-2-hydroxy-5-methoxybenzyl alcohol (**13**) using several methods.

Firstly we used the reaction of paraformaldehyde with a mixture of phenol and excess of boric acid in xylene. This method was developed by Yang[46] and allows yielding *o*-hydroxybenzyl alcohols in a good yield. However, this method requires a lot of manipulations and drastic conditions. The first step of this reaction is formation of boroxine which takes place by heating of the corresponding phenol and boric acid at 180 °C for 24 hours under conditions of continuous azeotropic distillation of water. After that paraformaldehyde is added to the reaction mixture and the reaction occurs at 80 °C for 24 hours. Unfortunately, following this protocol we have not reached desirable product because of decomposition of the starting material.

The second route which we have followed to synthesize the 3-fluoro-2-hydroxy-5-methoxybenzyl alcohol (**13**) required use of the paraformaldehyde in the presence of diethylaluminium chloride[47] (**Scheme 17**).

Scheme 17

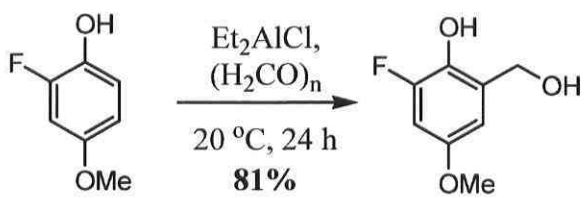

12 **13**

This reaction proceeds smoothly at 20 °C for 24 hours by undergoing of 2-fluoro-4-methoxyphenol (**12**) with 5.0 equivalents of paraformaldehyde and 1.5 equivalents of 1M Et_2AlCl in dichloromethane. The yield of 3-fluoro-2-hydroxy-5-methoxybenzyl alcohol (**13**) is 81% after purification by column chromatography.

This method has been developed by Sartori[48] group which is the general tactic for C-ortho regiospecific elaboration of variety of aromatic molecules via the electrophilic

aromatic substitution. The reaction key lies in the intermediacy of a quite rigid chelate transition state (**Scheme 18**) in which the aluminum plays the role of Lewis acid promoter and serves two functions: activation of the carbonyl carbon by coordination and regiocontrol of the process by keeping the reacting sites of the two reactants, i.e. carbonyl carbon atom of formaldehyde and ortho-carbon of phenol, into proximity.

Scheme 18

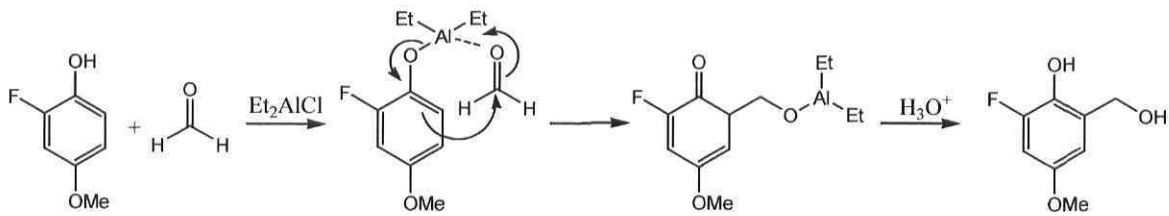

The next step of the synthesis is the selective protection of phenolic OH in the presence of primary hydroxyl group in 3-fluoro- 2-hydroxy-5-methoxybenzyl alcohol (**13**) (**Scheme 19**):

Scheme 19

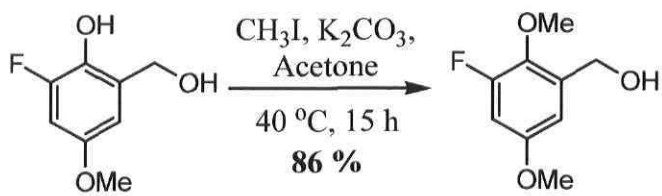

13 **14**

3-Fluoro-2-hydroxy-5-methoxybenzyl alcohol (**13**) was placed with 2.0 equivalents of K_2CO_3 and 4.0 equivalents of CH_3I in acetone. The reaction mixture was warmed to 40 °C for 15 hours. After that the inorganic layer was filtered and the product was subjected

to column chromatography to yield 3-fluoro-2,5-dimethoxybenzyl alcohol (**14**) in excellent yield (86%).

The next step of the synthesis is the transformation of 3-fluoro-2,5-dimethoxybenzyl alcohol (**14**) into the corresponding alkyl bromide (**15**) (**Scheme 20**).

Scheme 20

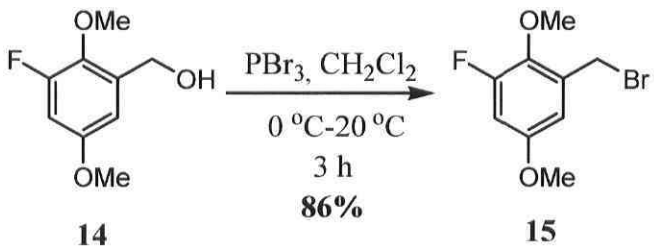

14 **15**

To a cooled (0 °C) solution of 3-fluoro-2,5 dimethoxybenzyl alcohol (**14**) in dichloromethane was added dropwise 1.5 equivalents of 1M PBr_3 in CH_2Cl_2. After 3 hours of reaction at 20 °C the solvent was evaporated and the product of the reaction was purified by column chromatography to get bromomethyl-3-fluoro-2,5-dimethoxybenzene (**15**) in 86% yield.

The two next steps include the incorporation of one more carbon in the side chain of the methylbromide-3-fluoro-2,5-dimethoxybenzene (**15**) and subsequent hydrolysis of obtained 3-fluoro-2,5-dimethoxyphenylacetonitrile (**16**) (**Scheme 21**).

Scheme 21

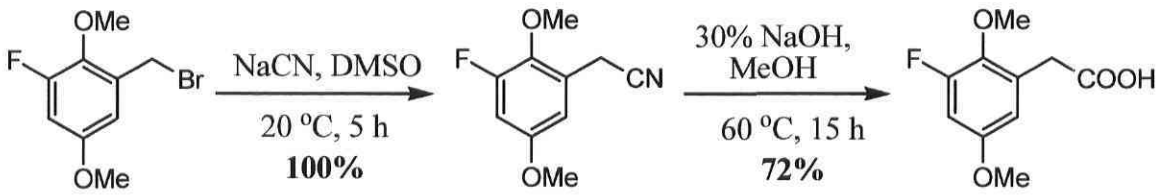

15 **16** **17**

The 3-fluoro-2,5-dimethoxyphenylacetonitrile (**16**) was obtained by undergoing of bromomethy-3-fluoro-2,5-dimethoxybenzene (**15**) with 2.0 equivalents of sodium cyanide in dimethylsulfoxide. This reaction smoothly proceeds under mildly conditions, (20 °C, 5 hours) with 100% yield.

To obtain 3-fluoro-2,5-dimethoxyphenylacetic acid (**17**), the 3-fluoro-2,5-dimethoxyphenylacetonitrile (**16**) was hydrolyzed under basic conditions using 30% aqueous solution of sodium hydroxide. We have again used the basic condition to avoid the lactone formation. The reaction lasted 15 hours at 60 °C with 72% yield of the product after chromatography.

The final step of the synthesis of 3-F HGA is the deprotection of two phenolic groups. For this we have followed the same protocol (**Scheme 22)** which we have used in the previous synthesis of 6-Cl HGA.

Scheme 22

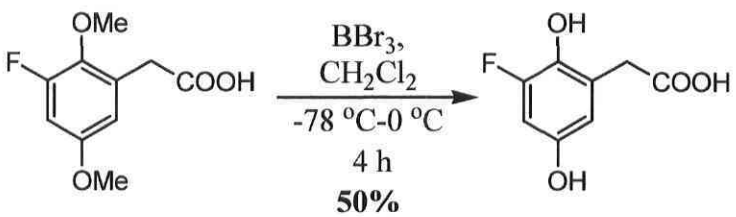

17 **18**

To 3-fluoro-2,5-dimethoxyphenylacetic acid (**17**) was added dropwise 3.3 equivalents of 1M BBr_3 in dichloromethane at -78 °C. After one hour the temperature was increased to 0 °C and after three hours the reaction was quenched with 5 ml of cold water. This time we have not managed to separate the forming lactone from the final product by washing the water layer with dichloromethane. The purification of product on a silica gel column has allowed yielding 3-fluoro-2,5-dihydroxyphenylacetic acid (**18**) in 50% yield.

Thus, the synthesis of 3-fluoro-2,5-dihydroxyphenylacetic acid (3-F HGA) (**18**) has been accomplished in 6 steps with 21.3% of overall yield.

Conclusion

The goal of this project is the synthesis of new inhibitors of human *homogentisate 1,2-dioxygenase* (HGO). These inhibitors belong to irreversible suicidal type and represent the halogenated analogues of the homogentisic acid, which is the substrate of HGO. These compounds may provide an alternate treatment for the fatal disease tyrosinemia type I.

We have synthesized two halogenated analogues of homogentisic acid: 6-chloro-2,5-dihydroxyphenylacetic acid (6-Cl HGA) (**9**) and 3-fluoro-2,5-dihydroxyphenylacetic acid (3-F HGA) (**18**).

The synthesis of 6-Cl HGA has been realized in eight steps and 12.5% overall yield. The chlorine incorporation in the desirable position of the benzene ring has been accomplished by Michael reaction of 2-(methoxycarbonyl)-1,4-benzoquinone (**2**) with HCl. We have improved this step using 2M solution of HCl in ether instead HCl gas [39] which has us allowed yielding methyl-6-chloro-2,5-dihydroxybenzoate (**3**) in a 70% of yield (versus 30% of yield in the case of using HCl gas).

The synthesis of 3-F HGA has been complited in six steps with an overall yield of 21.3%. The key-step of this synthesis was the ortho-specific hydroxymethylation of 2-fluoro-4-methoxyphenol (**12**) via the electrophilic aromatic substitution. This reaction has been accomplished by undergoing of 2-flouro-4-methoxyphenol (**12**) with paraformaldehyde in the presence of Et_2AlCl as a Lewis acid promoter and has allowed yielding the 3-fluoro-2-hydroxy-5-methoxybenzyl alcohol (**13**) in 81% of yield.

At present time, these two compounds are being tasted the inhibitory activity in laboratory of Lindsay D. Eltis at university of British Columbia.

Experimental Section

General Remarks

Starting materials and solvents were purchased from Aldrich Chemical Co. and used without further purification. The 2-fiuoro-4-hydroxyphenol was purchased from Apollo Scientific Ltd.

The anhydrous solvents were freshly prepared by distillation before every reaction. The tetrahydrofuran was distilled under argon atmosphere in the presence of sodium wire and the benzophenone as an indicator. The dichloromethane was distilled under argon atmosphere in the presence of CaH_2. The ether was distilled under argon atmosphere in the presence of $LiAlH_4$. The acetone was distilled under argon atmosphere in the presence of molecular sieves (4 Å, 3.2 mm pellets) previously activated by heating in a drying oven for 24 hours.

All reactions were performed in standard glass apparatus. For the reaction sensible to humidity the flasks were previously flamed under nitrogen atmosphere. The reagents and the anhydrous solvent were added into reaction system with the help of syringe through the septum. The reactions at 0 °C were realized with the help of a cooler, the reactions at -78 °C were realized using the bath from dry ice/acetone mixture.

The column flash-chromatography was performed on silica gel (Silicycle, 40-63 μm). The analytical thin layer chromatography (TLC) was performed using the glass plates covered with silica gel 60 F_{254} (Merck, layer thickness 250 μm). The visual detection of the thin layer chromatography was realized with the help of UV absorption and using of aqueous solution of cerium ammonium molybdate (CAM).

The characterization of the compounds was established by ^{1}H, ^{13}C NMR, IR spectroscopy and additionally by melting points. ^{1}H and ^{13}C NMR-spectra were recorded on a Varian Inova 400 MHz instrument; IR spectra were recorded on a BOMEM MB-100 instrument. Melting points of the solid compounds were determined on Fisher-Johns Melting Point apparatus. For the new compounds the elemental analysis was carried at Guelph Chemical Laboratories, Ltd in Ontario.

2-(Methoxycarbonyl)-1,4-benzoquinone (2)

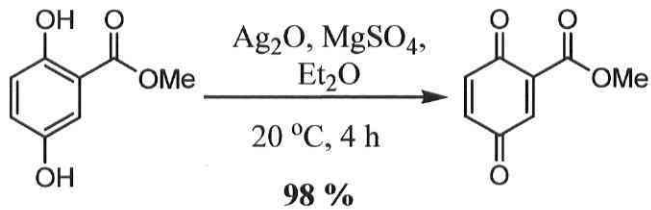

1 **2**

In an oven-dried 500 ml round-bottomed flask with a magnetic stirring bar was placed 6.00 g (35.68 mmol, 1.0 equiv) of methyl-2,5-dihydroxybenzoate (**1**) in 100 ml of Et_2O. Then 12.84 g of $MgSO_4$ (107.04 mmol, 3.0 equiv) and 12.40 g (53.52 mmol, 1.5 equiv) of freshly prepared Ag_2O were added. The reaction mixture was stirred at 20 °C for 4 hours. The colorless solution became orange. Then the inorganic residue was filtered and the ether solution was evaporated under reduced pressure to give 5.86 g of 2-(methoxycarbonyl)- 1,4-benzoquinone (**2**) as the orange crystals.

Yield 98%

Mp. 53-54 °C (Lit.[49] 53.5-54 °C)

^{1}H NMR (400 MHz, $CDCl_3$) δ (ppm) 3.87 (s, 3H), 6.79 (d, 1H, J 0.8 Hz), 6.80 (s, 1H), 7.07 (d, 1H, J 2.4 Hz)

^{13}C NMR (100 MHz, $CDCl_3$) δ (ppm) 53.1, 136.2, 136.5, 136.9, 137.0, 163.1, 183.0, 186.9

Preparation of Ag_2O[50]

To an aqueous solution (50 ml) of $AgNO_3$ (12.24 g, 72.05 mmol, 1.0 equiv) was added 2.88 g (72.00 mmol, 1.0 equiv) of NaOH dissolved in water (50 ml). The precipitated silver oxide was filtered, and then was washed twelve times with water, six times with acetone, and six times with anhydrous ether and was placed in the reaction immediately.

Methyl 6-chloro-2,5-dihydroxybenzoate (3)

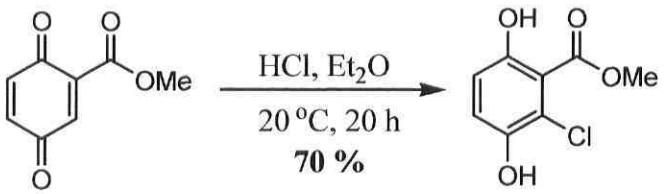

2 **3**

In an oven-dried 500 ml round-bottomed flask with a magnetic stirring bar was placed 7.60 g (45.75 mmol, 1.0 equiv) of 2-(methoxycarbonyl)-1,4-benzoquinone (**2**) in 130 ml Et_2O, then 80 ml (160.12 mmol, 3.5 equiv) of 2M solution of HCl in Et_2O was added and reaction mixture was stirred at 20 °C for 20 hours. The orange solution became yellow. Then the solvent was evaporated under reduced pressure and the residue was subjected to column chromatography. The product was eluted with hexane/ether (5/1) mixture. The obtained solid was recrystallized from hexane/ether mixture to give 6.53 g of methyl 6-chloro-2,5-dihydroxybenzoate (**3**) as white needle-shape crystals.

Yield 70%

Mp. 133 °C (Lit.[39] 131 °C)

R_f 0.62 (hexane/EtOAc 1/1)

^{1}H NMR (400 MHz, $CDCl_3$) δ (ppm) 4.09 (s, 3H), 6.98 (d, 1H, J 9.2 Hz), 7.25 (d, 1H, J 9.2 Hz)

^{13}C NMR (100 MHz, $CDCl_3$) δ (ppm) 52.9, 111.0, 117.9, 118.2, 122.8, 145.5, 157.0, 169.9

IR (KBr, cm^{-1}) 3439, 3031, 1665, 1590, 1443

6-Chloro-2,5-dihydroxybenzyl alcohol (4)

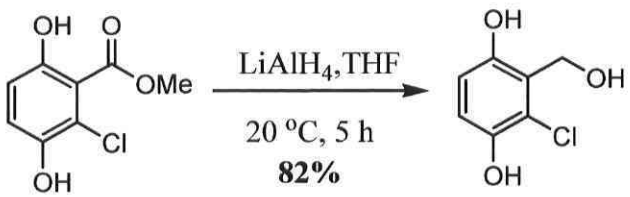

3 **4**

In an oven-dried 500 ml round-bottomed flask with a magnetic stirring bar was placed 2.45 g of $LiAlH_4$ (64.46 mmol, 2.0 equiv), then 100 ml of anhydrous Et_2O was added at 0 °C and under nitrogen atmosphere. Then 6.53 g (32.23 mmol, 1.0 equiv) of methyl 6-chloro-2,5-dihydroxybenzoate (**3**) in 150 ml of anhydrous THF was added dropwise, a cold bath was removed and reaction mixture was stirred at 20 °C for 5 hours. After that the reaction mixture was again cooled down to 0 °C, 20 ml of saturated NH_4Cl and 5 ml of 10%-HCl were added, then organic layer was separated from inorganic precipitate. The organic layer was dried over $MgSO_4$, the solvent was evaporated under reduced pressure, and the dark yellow residue was subjected to column chromatography. The product was eluted with hexane/EtOAc (10/4) mixture. The obtained solid was recrystallized from hexane/EtOAc mixture to give 4.58 g of 6-chloro-2,5-dihydroxybenzyl alcohol (**4**) as rose needle-shape crystals.

Yield 82%

M.p. 128-129 °C (Lit.[51] 128-129 °C)

R_f 0.61 (hexane/EtOAc 1/1)

^{1}H NMR (400 MHz, CD_3OD) δ (ppm) 4.79 (s, 2H), 6.61 (d, 1H, J 8.8 Hz), 6.72 (d, 1H, J 8.8 Hz)

^{13}C NMR (100 MHz, CD_3OD) δ (ppm) 58.4, 115.5, 117.2, 122.6, 126.3, 147.3, 151.2

IR (KBr, cm^{-1}) 3500, 3380, 3000, 2905, 1607, 1472, 1446, 1289, 1265, 1198, 990, 845

6-Chloro-2,5-dimethoxybenzyl alcohol (5)

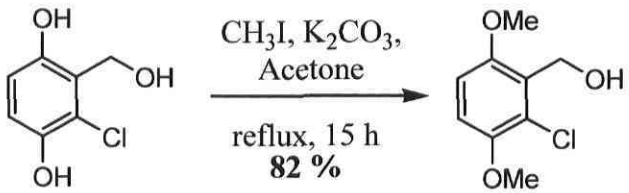

4 **5**

In an oven-dried 250 ml round-bottomed flask with a magnetic stirring bar was placed 1.78 g (10.20 mmol, 1.0 equiv) of 6-chloro-2,5-dihydroxybenzyl alcohol (**4**) in 100 ml of anhydrous acetone, then 3.00 g (20.40 mmol, 2.0 equiv) of K_2CO_3 and 1.3 ml (20.40 mmol, 2.0 equiv) of CH_3I were added. The reaction mixture was heated at reflux for 15 hours. After that the inorganic layer was filtered and the solvent was evaporated under reduced pressure. The obtained residue was subjected to column chromatography. The product was eluted with hexane/EtOAc (10/3) mixture. The obtained solid was recrystallized from hexane-EtOAc mixture to give 1.68 g of 6-chloro-2,5-dimethoxybenzyl alcohol (**5**) as white plate-shape crystals.

Yield 82%

M.p. 115 °C

R_f 0.5 (hexane/EtOAc 1/1)

^{1}H NMR (400 MHz, $CDCl_3$) δ (ppm) 3.83 (s, 3H), 3.84 (s, 3H), 4.88 (s, 2H), 6.76 (d, 1H, J 9.2 Hz), 6.84 (d, 1H, J 9.2 Hz)

^{13}C NMR (100 MHz, $CDCl_3$) δ (ppm) 56.4, 57.0, 58.2, 109.4, 111.9, 123.8, 128.5, 149.8, 152.8

IR (KBr, cm^{-1}) 2959, 2838, 1817, 1582, 1482, 1468, 1258, 1175, 1150, 807, 601

Elemental analysis:

Formula: $C_9H_{11}ClO_3$

Molecular mass: 202.64

Calculated: C, 53.34; H, 5.47; Cl, 17.50

Found: C, 53.03; H, 5.30; Cl, 17.79

Bromomethyl-6-chloro-2,5-dimethoxybenzene (6)

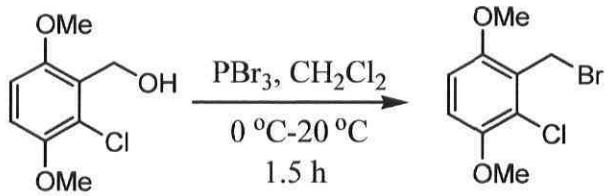

5 6

To a cooled to 0 °C solution of 6-chloro-2,5-dimethoxybenzyl alcohol (**5**) (1.39 g, 6.86 mmol, 1.0 equiv) in 30 ml of CH_2Cl_2 was added dropwise 10.30 ml (10.29 mmol, 1.5 equiv) of 1M PBr_3 in CH_2Cl_2 under nitrogen atmosphere. Then reaction mixture was stirred at 20 °C for 1.5 hours. Then the reaction mixture was poured into water. The organic layer was separated, dried over $MgSO_4$ and the solvent was evaporated under reduced pressure. The obtained residue was subjected to column chromatography. The product was eluted with hexane/EtOAc (10/1.5) mixture. The obtained light yellow oil of bromomethyl-6-chloro-2,5-dimethoxybenzene (**6**) (1.54 g) was crystallized in the white solid after standing at room temperature for 5-10 min.

Yield 83%

M.p. 69 °C

R_f 0.77 (hexane/EtOAc 1/1)

^{1}H NMR (400 MHz, $CDCl_3$) δ (ppm) 3.86 (s, 3H), 3.87 (s, 3H), 4.73 (s, 2H), 6.76 (d, 1H, J 9.2 Hz), 6.87 (d, 1H, J 9.2 Hz)

^{13}C NMR (100 MHz, $CDCl_3$) δ (ppm) 25.6, 56.6, 57.0, 109.6, 112.8, 124.5, 126.1, 149.8, 152.4

IR (KBr, cm^{-1}) 3057, 2999, 2834, 1582, 1483, 1278, 1262, 1219, 1182, 1052, 806

Elemental analysis:

Formula:	$C_9H_{10}BrClO_2$
Molecular mass:	265.53
Calculated:	C, 40.71; H, 3.74; Br, 30.09; Cl, 13.35
Found:	C, 41.03; H, 3.65; Br, 29.94; Cl, 13.69

6-Chloro-2, 5-dimethoxyphenylacetonitrile (7)

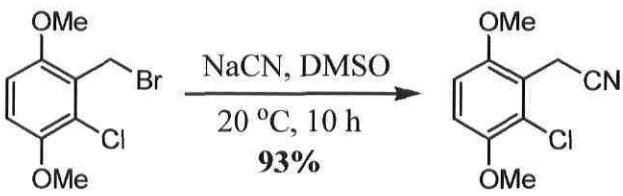

6 **7**

In an oven-dried 250 ml round-bottomed flask with a magnetic stirring bar was placed 1.40 g (5.27 mmol, 1.0 equiv) of bromomethyl-6-chloro-2,5-dimethoxybenzene (**6**) in 10 ml of DMSO, then 0.39 g (7.91 mmol, 1.5 equiv) NaCN was added. The reaction mixture was stirred at 20 °C for 10 hours. After that 15 ml of EtOAc was added in reaction mixture, then it was washed with water (5x10 ml), the organic layer was dried over $MgSO_4$ and solvent was evaporated under reduced pressure. The obtained oil was subjected to column chromatography. The product was eluted with hexane/EtOAc (10/3) mixture. The obtained solid was recrystallized from hexane/Et_2O mixture to give 1.36 g of 6-chloro-2,5-dimethoxyphenylacetonitrile (**7**) as white needle-shape crystals.

Yield 93%

M.p. 81 °C

R_f 0.6 (hexane/EtOAc 1/1)

^1H NMR (400 MHz, $CDCl_3$) δ (ppm) 3.85 (s, 3H), 3.86 (s, 5H), 6.79 (d, 1H, J 9.2 Hz), 6.89 (d, 1H, J 9.2 Hz)

^{13}C NMR (100 MHz, $CDCl_3$) δ (ppm) 16.0, 56.5, 57.0, 109.4, 112.4, 117.2, 119.1, 124.1, 149.8, 152.0

IR (KBr, cm^{-1}) 3092, 2970, 2841, 2245, 1585, 1490, 1263, 1214, 1032, 807

Elemental analysis:

Formula:	$C_{10}H_{10}ClNO_2$
Molecular mass:	211.65
Calculated:	C, 56.75; H, 4.76; N, 6.62
Found:	C, 57.14; H, 4.55; N, 6.59

6-Chloro-2,5-dimethoxyphenylacetic acid (8)

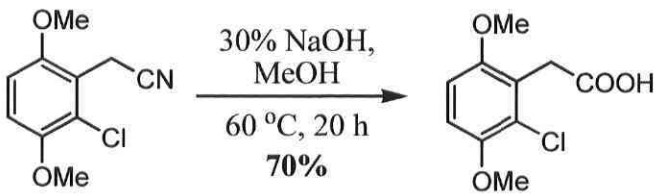

7 **8**

In an oven-dried 250 ml round-bottomed flask with a magnetic stirring bar was placed 1.15 g (5.43 mmol, 1.0 equiv) of 6-chloro-2,5-dimethoxyphenylacetonitrile (**7**) in 15 ml of MeOH, then 10 ml of 30% NaOH was added and reaction mixture was heated to 60 °C for 20 hours. After that the reaction mixture was cooled down to 0 °C, 10% HCl was added to pH~5 and eluted with EtOAc. The organic layer was washed with brine and water, then dried over $MgSO_4$ and solvent was evaporated under reduced pressure. The obtained residue was subjected to column chromatography. The product was eluted with hexane/EtOAc (2/1) mixture. The obtained solid was recrystallized from hexane/EtOAc mixture to give 0.81 g of 6-chloro-2,5-dimethoxyphenylacetic acid (**8**) as white snowflake-shape crystals.

Yield 70%

M.p. 199-200 °C

R_f 0.13 (hexane/EtOAc 1/1)

^{1}H NMR (400 MHz, $CDCl_3$) δ (ppm) 3.79 (s, 3H), 3.86 (s, 3H), 3.92 (s, 2H), 6.77 (d, 1H, J 9.2 Hz), 6.84 (d, 1H, J 9.2 Hz)

^{13}C NMR (100 MHz, $CDCl_3$) δ (ppm) 33.6, 56.8, 57.2, 110.5, 112.5, 124.9, 125.4, 151.0, 154.0, 174.7

IR (KBr, cm^{-1}) 3011, 2938, 2838, 1724, 1696, 1583, 1482, 1434, 1265, 1241, 968, 640

6-Chloro-2,5-dihydroxyphenylacetic acid (9)

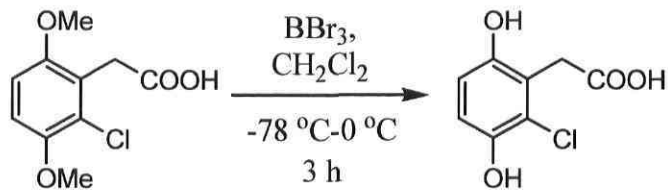

8 **9**

In an oven-dried 250 ml round-bottomed flask with a magnetic stirring bar was placed 0.45 g (1.95 mmol, 1.0 equiv) of 6-chloro-2,5-dimethoxyphenylacetic acid (**8**) in 30 ml of anhydrous CH_2Cl_2 under nitrogen atmosphere. Then reaction mixture was cooled down to -78 °C and 5.0 ml (4.88 mmol, 2.5 equiv) of 1M BBr_3 in CH_2Cl_2 was added dropwise. After 1 hour, the temperature of the reaction was increased to 0 °C and the reaction mixture was stirred at this temperature for 2 hours. After that 10 ml of the cold water was added, the organic layer was removed from water one. The organic layer was washed with water (5x5 ml). The water fractions were combined, extracted with EtOAc (5x6 ml), then EtOAc-layer was dried over $MgSO_4$ and evaporated under reduced pressure. The obtained light yellow oil was subjected to column chromatography. The product was eluted with EtOAc to give 0.20 g of 6-chloro-2,5-dihydroxyphenylacetic acid (**9**) as a rose powder.

Yield 50%

M.p. 175-176 °C

R_f 0.84 (hexane/EtOAc 1/1)

^{1}H NMR (400 MHz, CD_3OD) δ (ppm) 3.78 (s, 2H), 6.61 (d, 1H, J 8.8 Hz), 6.70 (d, 1H, J 8.8 Hz)

^{13}C NMR (100 MHz, CD_3OD) δ (ppm) 33.8, 114.8, 116.3, 122.4, 123.3, 147.3, 150.7, 175.2

IR (KBr, cm^{-1}) 3364, 2637, 1705, 1686, 1497, 1395, 1263, 1229, 963, 810

Elemental analysis:

Formula:	$C_8H_7ClO_4$
Molecular mass:	202.59
Calculated:	C, 47.43; H, 3.49
Found:	C, 47.68; H, 3.17

3-Fluoro-2-hydroxy-5-methoxybenzyl alcohol (13)

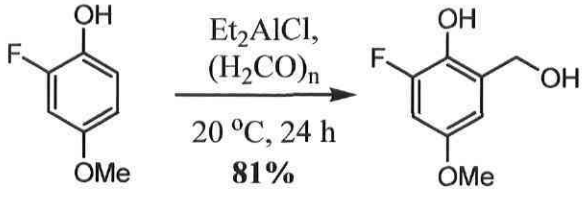

12 **13**

In an oven-dried 250 ml round-bottomed flask with a magnetic stirring bar were placed 1.00 g (7.04 mmol, 1.0 equiv) of 2-fluoro-4-methoxyphenol (**12**) and 1.05 g (35.20 mmol, 5.0 equiv) of paraformaldehyde in 30 ml of anhydrous CH_2Cl_2. Then the reaction mixture was cooled down to 0 °C and 11 ml (10.56 mmol, 1.5 equiv) of 1M Et_2AlCl in CH_2Cl_2 was added dropwise under nitrogen atmosphere. After that the cool bath was removed and the reaction mixture was stirred at 20 °C for 24 hours. After that 15 ml of 10% HCl was added, the unsolved residue was removed using celite. The CH_2Cl_2-layer was separated from water one, the water layer was extracted with EtOAc (5x10 ml); the organic fractions were combined, dried over $MgSO_4$ and evaporated under reduced pressure. The obtained brown oil was subjected to column chromatography. The product was eluted with hexane/Et_2O (10/3) mixture. The obtained solid was recrystallized from CH_2Cl_2/ Et_2O mixture to give 0.97 g of 3-fluoro-2-hydroxy-5-methoxybenzyl alcohol (**13**) as white needle-shape crystals.

Yield 81%

M.p. 66-67 °C

R_f 0.68 (hexane/EtOAc 1/1)

^{1}H NMR (400 MHz, $CDCl_3$) δ (ppm) 3.73 (s, 3H), 4.75 (s, 2H), 6.47 (dd, 1H, $^4J_{H4,H6}$ 2.8 Hz, $^3J_{H4,F}$ 14 Hz), 6.65 (dd, 1H, $^4J_{H6,H4}$ 2.8 Hz, $^5J_{H6,F}$ 0.8 Hz)

^{13}C NMR (100 MHz, $CDCl_3$) δ (ppm) 56.1 (s, OCH_3), 62.8 (d, $^5J_{C-F}$ 12.8 Hz, CH_2OH), 102.0 (d, $^2J_{C-F}$ 87.2 Hz, C-4), 108.8 (d, $^4J_{C-F}$ 10.4 Hz, C-6), 128.6 (d, $^3J_{C-F}$ 12.8 Hz, C-1),

136.6 (d, $^{2}J_{C-F}$ 56.4 Hz, C-2), 151.6 (d, $^{1}J_{C-F}$ 1104.8 Hz, C-3), 152.8 (d, $^{3}J_{C-F}$ 115.6 Hz, C-5).

IR (KBr, cm^{-1}) 3362, 1632, 1598, 1497, 1504, 1476, 1339, 1219, 1196, 963, 940, 840, 764

Elemental analysis:

Formula:	$C_8H_9FO_3$
Molecular mass:	172.16
Calculated:	C, 55.82; H, 5.27; F, 11.03
Found:	C, 56.20; H, 5.51; F, 10.69

3-Fluoro-2,5-dimethoxybenzyl alcohol (14)

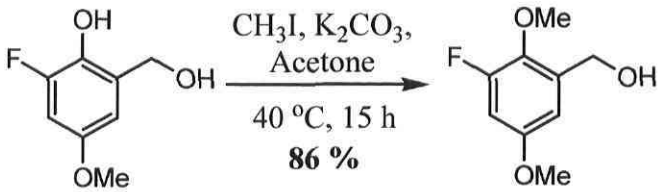

13 **14**

In an oven-dried 250 ml round-bottomed flask with a magnetic stirring bar was placed 1.00 g (5.81 mmol, 1.0 equiv) of 3-fluoro-2-hydroxy-5-methoxybenzyl alcohol (**13**) in 50 ml of anhydrous acetone, then 1.66 g (11.62 mmol, 2.0 equiv) of K_2CO_3 and 1.5 ml (23.24 mmol, 4.0 equiv) of CH_3I were added. The reaction mixture was warmed to 40 °C for 15 hours. After that the inorganic layer was filtered and the solvent was evaporated under reduced pressure. The obtained residue was subjected to column chromatography. The product was eluted with hexane/Et_2O (10/4) mixture. The obtained solid was recrystallized from hexane/Et_2O mixture to give 0.96 g of 3-fluoro-2,5-dimethoxybenzyl alcohol (**14**) as white needle-shape crystals.

Yield 86%

M.p. 43 °C

R_f 0.67 (hexane/EtOAc 1/1)

^{1}H NMR (400 MHz, $CDCl_3$) δ (ppm) 3.76 (s, 3H), 3.88 (s, 3H), 4.67 (s, 2H), 6.56 (dd, 1H, $^4J_{H4,H6}$ 3.2 Hz, $^5J_{H6,F}$ 13.2 Hz), 6.67 (m, 1H)

^{13}C NMR (100 MHz, $CDCl_3$) δ (ppm) 55.9 (s, OCH_3), 61.3 (d, $^6J_{C\text{-}F}$ 12.8 Hz, OCH_3), 61.8 (d, $^5J_{C\text{-}F}$ 20.8 Hz, CH_2OH), 102.5 (d, $^4J_{C\text{-}F}$ 90 Hz, C-6), 108.9 (d, $^2J_{C\text{-}F}$ 12 Hz, C-4), 135.8 (d, $^2J_{C\text{-}F}$ 12.8, C-2), 139.1 (d, $^3J_{C\text{-}F}$ 52 Hz, C-1), 155.7 (d, $^1J_{C\text{-}F}$ 982 Hz, C-3), 155.8 (d, ^{3}J 408.0 Hz, C-5)

IR (KBr, cm^{-1}) 3250, 2950, 2841, 1620, 1496, 1229, 1140, 1003, 972, 962, 824

Elemental analysis:

Formula:	$C_9H_{11}FO_3$
Molecular mass:	186.12
Calculated:	C, 58.06; H, 5.96; F, 10.20
Found:	C, 58.32; H, 6.16; F, 10.20

Bromomethyl-3-fluoro-2,5-dimethoxybenzene (15)

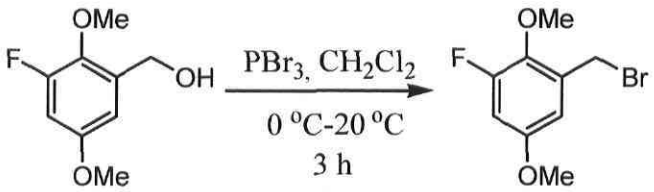

14 **15**

To a cooled (0 °C) solution of 1.30 g (6.98 mmol, 1.0 equiv) of 3-fluoro-2,5-dimethoxybenzyl alcohol (**14**) in anhydrous CH_2Cl_2 (20 ml) was added dropwise 10 ml (10.47 mmol, 1.5 equiv) of 1M PBr_3 in CH_2Cl_2 under nitrogen atmosphere. Then reaction mixture was stirred at 20 °C for 3 hours. Then the reaction mixture was poured into water. The organic layer was separated, dried over $MgSO_4$ and the solvent was evaporated under reduced pressure. The obtained residue was subjected to column chromatography. The product was eluted with hexane/Et_2O (10/1) mixture. The obtained colorless oil was crystallized in the white solid in the fridge to give 1.50 g of bromomethyl-3-fluoro-2,5-dimethoxybenzene (**15**).

Yield 86%

M.p. 29 °C

R_f 0.30 (hexane/EtOAc 1/2)

^{1}H NMR (400 MHz, $CDCl_3$) δ (ppm) 3.77 (s, 3H), 3.96 (s, 3H), 4.50 (s, 2H), 6.61 (dd, 1H, $^4J_{H4,H6}$ 2.8 Hz, $^3J_{H4,F}$ 14.0 Hz), 6.65 (dd, 1H, $^4J_{H4,H6}$ 2.8 Hz, $^5J_{H6,F}$ 14.0 Hz)

^{13}C NMR (100 MHz, $CDCl_3$) δ (ppm) 27.6 (d, $^5J_{C-F}$ 16 Hz, CH_2OH), 55.9 (s, OCH_3), 61.9 (d, $^6J_{C-F}$ 20 Hz, OCH_3), 104.1 (d, $^2J_{C-F}$ 88 Hz, C-4), 110.7 (d, $^4J_{C-F}$ 8 Hz, C-6), 132.9 (d, $^3J_{C-F}$ 16 Hz, C-1), 139.9 (d, $^2J_{C-F}$ 48.8 Hz, C-2), 155.6 (d, $^3J_{C-F}$ 41.2 Hz, C-5), 156.0 (d, $^1J_{C-F}$ 984.0 Hz, C-3)

IR (KBr, cm^{-1}) 2946, 1621, 1592, 1499, 1444, 1342, 1244, 1147, 104

Elemental analysis:

Formula:	$C_9H_{10}BrFO_2$
Molecular mass:	249.08
Calculated:	C, 43.40; H, 4.05; F, 7.63
Found:	C, 43.37; H, 4.21; F, 7.90

3-Fluoro-2, 5-dimethoxyphenylacetonitrile (16)

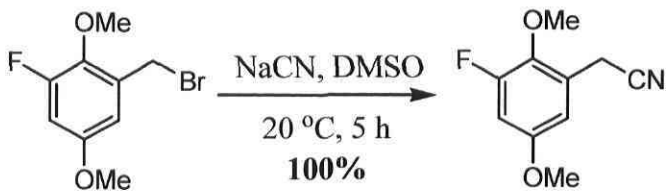

15 **16**

In an oven-dried 250 ml round-bottomed flask with a magnetic stirring bar was placed 1.20 g (4.82 mmol, 1.0 equiv) of bromomethyl-3-fluoro-2,5-dimethoxybenzene (**15**) in 20 ml of DMSO, then 0.48 g (9.64 mmol 2.0 equiv) NaCN was added. The reaction mixture was stirred at 20 °C for 15 hours. After that 15 ml of water was added in the reaction mixture, then it was extracted with EtOAc (5x5 ml), the organic layer was dried over $MgSO_4$ and solvent was evaporated under reduced pressure. The obtained yellow oil was subjected to column chromatography. The product was eluted with hexane/Et_2O (10/1.5) mixture. The obtained colorless oil was crystallized in the fridge to give 0.96 g of 3-fluoro-2,5-dimethoxyphenylacetonitrile (**16**) as a white solid product.

Yield 100%

M.p. 38 °C

R_f 0.53(hexane/EtOAc 1/2)

^{1}H NMR (400 MHz, $CDCl_3$) δ (ppm) 3.70 (s, 2H), 3.77 (s, 3H), 3.92 (d, 3H, $J_{H,F}$ 1.6 Hz, OCH_3 at C-2), 6.62 (d, 1H, J=3.2 Hz), 6.67 (ls, 1H)

^{13}C NMR (100 MHz, $CDCl_3$) δ (ppm) 18.9 (d, $^5J_{C\text{-}F}$ 12 Hz, CH_2OH), 56.1 (s, OCH_3), 61.6 (d, $^6J_{C\text{-}F}$ 24 Hz, OCH_3), 103.4 (d, $^2J_{C\text{-}F}$ 92 Hz, C-4), 109.9 (d, $^4J_{C\text{-}F}$ 12 Hz, C-6), 117.7 (s, CN), 125.2 (d, $^3J_{C\text{-}F}$ 16 Hz, C-1), 139.2 (d, $^2J_{C\text{-}F}$ 48 Hz, C-2), 155.7 (d, $^1J_{C\text{-}F}$ 984.0 Hz, C-3), 155.8 (d, $^3J_{C\text{-}F}$ 43.6 Hz, C-4)

IR (KBr, cm^{-1}) 2951, 2253, 1627, 1594, 1504, 1246, 1230, 1195, 825

Elemental analysis:

Formula:	$C_{10}H_{10}FNO_2$
Molecular mass:	195.19
Calculated:	C, 61.53; H, 5.16; F, 9.73
Found:	C, 61.71; H, 5.41; F, 9.56

3-Fluoro-2,5-dimethoxyphenylacetic acid (17)

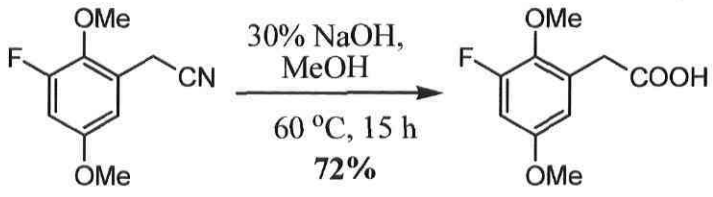

16 **17**

In an oven-dried 250 ml round-bottomed flask with a magnetic stirring bar was placed 0.91 g (4.66 mmol, 1.0 equiv) 3-fluoro-2,5-dimethoxyphenylacetonitrile (**16**) in 30 ml of MeOH, then 10 ml of 30% NaOH was added and reaction mixture was heated to 60 °C for 15 hours. After that the reaction mixture was cooled down to 0 °C, 10% HCl was added to pH~5 and eluted with EtOAc. The organic layer was washed with brine and water, then dried over $MgSO_4$ and evaporated under reduced pressure. The obtained dark yellow oil was subjected to column chromatography. The product was eluted with hexane/Et_2O (10/3) mixture. The obtained yellow solid was recrystallized from hexane/Et_2O mixture to give 0.72 g white plate-shape crystals of 3-fluoro-2,5-dimethoxyphenylacetic acid (**17**).

Yield 72%

M.p. 91-92 °C

R_f 0.89 (hexane/EtOAc 3/1)

^{1}H NMR (400 MHz, CD_3OD) δ (ppm) 3.61 (s, 2H), 3.74 (s, 3H), 3.81 (d, 3H, $J_{H,F}$ 1.2 Hz, OCH_3 at C-2), 6.61 (dd, 1H, $^3J_{H4,H6}$ 2.8 Hz, $^4J_{H6,F}$ 1.6 Hz), 6.66 (dd, 1H, $^3J_{H4,H6}$ 2.8 Hz, $^2J_{H4,F}$ 12.8 Hz).

^{13}C NMR (100 MHz, CD_3OD) δ (ppm) 36.5 (d, $^5J_{C-F}$ 12 Hz, CH_2), 56.34 (s, OCH_3), 61.8 (d, $^6J_{C-F}$ 20 Hz, OCH_3), 103.0 (d, $^2J_{C-F}$ 92 Hz, C-4), 112.7 (d, $^4J_{C-F}$ 8Hz, C-6), 131.6 (d, $^3J_{C-F}$ 16 Hz, C-1), 141.1 (d, $^2J_{C-F}$ 48 Hz, C-2), 157.1 (d, $^3J_{C-F}$ 43.6 Hz, C-5), 157.3 (d, $^1J_{C-F}$ 974 Hz, C-3), 175.23

IR (KBr, cm^{-1}) 3008, 1719, 1696, 1503, 1334, 1234, 1203, 834, 626

Elemental analysis:

Formula:	$C_{10}H_{11}FO_4$
Molecular mass:	214.19
Calculated:	C, 56.08; H, 5.18; F, 8.87
Found:	C, 56.48; H, 5.49; F, 8.62

3-Fluoro-2,5-dihydroxyphenylacetic acid (18)

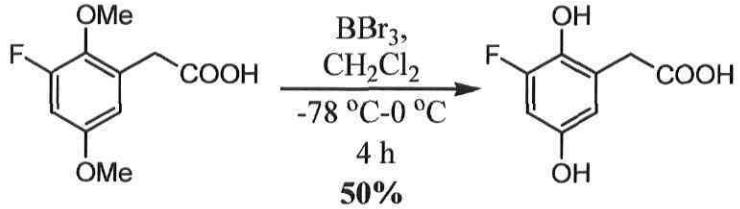

17 **18**

In an oven-dried 250 ml round-bottomed flask with a magnetic stirring bar was placed 0.60 g (2.80 mmol, 1.0 equiv) of 3-fluoro-2,5-dimethoxyphenylacetic acid (**17**) in 25 ml of anhydrous CH_2Cl_2. Then the reaction mixture was cooled down to -78 °C and 8.5 ml (9.24 mmol, 3.3 equiv) of 1M BBr_3 in CH_2Cl_2 was added dropwise under nitrogen atmosphere. After 1 hour the temperature of the reaction was increased to 0 °C and the reaction mixture was stirred at 0 °C for 3 hours. After that 10 ml of the cold water was added, the organic layer was removed from the water one. The organic layer was washed with water (5x5 ml). The water fractions were combined, extracted with EtOAc (5x6 ml), then EtOAc-layer was dried over $MgSO_4$ and evaporated under reduced pressure. The obtained light yellow oil was subjected to column chromatography. The product was eluted with hexane/EtOAc (1/2) mixture to give 0.26 g of 3-fluoro-2,5-dihydroxyphenylacetic acid (**18**) as rose powder.

Yield 50%

M.p. 153 °C

R_f 0.87 (hexane/EtOAc 1/1)

^{1}H NMR (400 MHz, acetone-d_6) δ (ppm) 3.62 (s, 2H), 6.54 (dd, 1H, $^3J_{H4,F}$ 9.6 Hz, $^4J_{H4,H6}$ 2.8 Hz), 6.51 (d, 1H, J 2.8 Hz)

^{13}C NMR (100 MHz, CD_3OD) δ (ppm) 36.4 (d, $^5J_{C-F}$ 12 Hz, CH_2), 103.2 (d, $^2J_{C-F}$ 88 Hz, C-4), 113.8 (d, $^3J_{C-F}$ 12 Hz, C-6), 126.4 (d, $^3J_{C-F}$ 16 Hz, C-1), 137.1 (d, $^2J_{C-F}$ 60 Hz, C-2), 151.2 (d, $^3J_{C-F}$ 42.8 Hz, C-5), 153.4 (d, $^1J_{C-F}$ 943.2 Hz, C-3), 175.7

IR (KBr, cm^{-1}) 3408, 1725, 1694, 1505, 1353, 1254, 1137, 791

The data of ^{1}H spectrum were in accord with those reported in the literature.[37]

References

1. Brownlee, J. M.; Kayunta, J.-W.; Harrison, D. H. T.; Moran, G. R. *Biochemistry*, **2004**, *43,* 6370-77.
2. Laberge, C.; Grenier, A.; Gagné, R. *Union Med. Canada*, **1981**, *110,* 621-25.
3. Al-Essa, M. A.; Rashed, M. S.; Ozand, P. T. *East. Med. Health J.*, **1999**, *5*, 1204-07.
4. Cerone, R.; Holme, E.; Schiaffino, M. C.; Caruso, U.; Maritano, L.; Romano, C. *Acta Paediatr.*, **1997**, *86,* 1013-15.
5. Kubo, S.; Kiwaki, K.; Awata, H.; Katoh, H.; Kanegae, Y.; Saito, I.; Yamamoto, T.; Miyazaki, J.; Matsuda, I.; Endo, F. *Hum. Gene Ther.* **1997**, *8*, 65-71.
6. Du, L. *Am. J. Hum. Genet.*, **1998**, *62,* 765-67.
7. Fernandez-Canon, J. M.; Penalva, M. A. *J. Biol. Chem.*, **1998**, *273*, 329-37.
8. Grompe, M.; St-Louis, M.; Demers, S. I.; Al-Dalimy, M.; Leclerc, B.; Tanguay, R. M. *N. Engl. J. Med.*, **1994**, *331*, 353-57.
9. Bussières, J. F; Mitchell, G. *Québec Pharmacie*, **1998**, *45*, 361-71.
10. Onodera, K. *Natural History*, **1988**, *1*, 1.
11. Baber, M. D. *Arch. Dis. Child.*, **1956**, *3,* 335-39.
12. Laberge, C. *Am. J. Hum. Genet.*, **1969**, *21*, 36-45.
13. Croffie, J. M.; Gupta, S. K.; Fitzgerald, C. *Pediatrics,* **1999**, *103,* 675-78.
14. Van Spronsen, F. J.; Thomasse, Y.; Smith, G. P. *Hepatology*, **1994**, *20,* 1187-91.
15. Sokal, E. M.; Bustos R.; Van Hoof F.; Otte J. B. *Transplantation,* **1992**, *54,* 937-39.
16. Laine, J.; Salo, K. M.; Krogerus, L.; Karkkainen, J.; Wahlroos, O.; Holmberg, C. *Pediatric Research*, **1995**, *37*, 640-45.
17. Lindstedt, S.; Holme, E.; Lock, E. A.; Hjalmarson, O.; Strandvik, B. *Lancet,* **1992**, *340*, 813-17.

18. Holme, E.; Lindstedt, S. *J. Inherit. Metab. Dis.*, **1998**, *21*, 507-17.

19. Paradis, K. *Clin. Invest. Med.*, **1996**, *19*, 311-16.

20. Kumar, A. *Handbook of Enzymes*, **2001**, ATPA.

21. Palmer Trevor, B. A. *Understanding Enzymes*, **1985**, Ellis Horwood Limited.

22. Bugg, T. D. H. *Introduction to Enzyme and Coenzyme Chemistry*, **2004**, Blackwell Publishing Ltd.

23. Fritz, I. M.; Linden, L.; Freigang, J.; Auerbach, G.; Huber, R.; Steinbacher, S. *Plant Physiology*, **2004**, *134*, 1388-1400.

24. http://alchemy.chem.uwm.edu/research/moran/grouppage/website/4HPPD.html

25. Lock, E. A.; Ellis, M. K.; Gaskin, P.; Robinson, M.; Auton, T. R.; Provan, W. M.; Smith, L. L.; Prisbylla, M. P.; Mutter, L. C.; Lee, D. L. *J. Inherit. Metab. Dis.*, **1998**, *21*, 498-506.

26. Matringe, M.; Sailland, A.; Pelissier, B.; Rolland, A.; Zink, O. *Pest. Manag. Sci.*, **2005**, *61*, 269-76.

27. Lin, S.-W.; Lin, Y.-L.; Lin, T.-C.; Yang, D.-Y. *Bioorg. Med. Chem. Lett.*, **2000**, *10*, 1297-98.

28. Lin, Y.-L.; Wu, C.-S.; Lin, S.-W.; Huang, J.-L.; Sun, Y.-S.; Yang, D.-Y. *Bioorg. Med. Chem.*, **2002**, *10*, 685-90.

29. Timm, D. E.; Mueller, H. A.; Bhanumoorthy, P.; Harp, J. M.; Bunick, G. J. *Structure*, **1999**, *7*, 1023-33.

30. Philips, M.; Kaplan, A.; Rutter, W.; Bartlett, P. A. *Biochemistry*, **1992**, *31*, 959-63.

31. Raynard, L. B.; Bhanumoorthy, P.; Witte, J. F.; McClard, R. W.; Grompe, M.; Timm, D. E. *J. Biol. Chem.*, **2001**, *276*, 15284-91.

32. Titus, G. P.; Mueller, H. A.; Burgner, J.; Córdoba, S. A.; Peñalva, M. A.; Timm, D. A. *Nat. Struct. Biol.*, **2000**, *7*, 542-546.

33. Fernández-Cañón, J. M.; Peñalva, M. A. *Proc. Natl. Acad. Sci. USA*, **1995**, *92*, 9132-36.

34. Vaillancourt, F. H.; Labbé, G.; Drouin, N. M.; Fortin, P. D.; Eltis, L. D. *J. Biol. Chem.*, **2002**, *277*, 2019-27.

35. Veldhuizen, E. J. A.; Vaillancoutr, F. H.; Whiting, C. J.; Hsiao, M. M.-Y.; Gingras, G.; Xiao, Y.; Tanguay, R. M.; Boukouvalas, J.; Eltis, L. D. *Biochem. J.*, **2005**, *386*, 305-314.

36. Hiyama, T. *Organofluorine Compounds. Chemistry and Applications*, **2000**, Springer-Verlag.

37. Robert, A.; Pascal, J.; Jack Chen, Y.-C. *Biochemistry*, **1985**, *24*, 3158-65.

38. Nakazaki, M.; Naemura, K. *J. Org. Chem.*, **1981**, *46*, 106-11.

39. Holmes, T. J.; John, V.; Venerstrom, J.; Choi, K. E. *J. Org. Chem.*, **1984**, *49*, 4736-38.

40. McMurry, J. E.; Erion, M. D. *J. Am. Chem. Soc.*, **1985**, *107*, 2712-20.

41. Clive, D. L. J.; Sannigrahi, M.; Hisaindee, S. *J. Org. Chem.*, **2001**, *66*, 954-61.

42. Norte, M.; Rodriguez, L.; Fernández, J.; Eguren, L.; Estrada, D. M. *Tetrahedron*, **1988**, *44*, 4973-80.

43. Layton, M. E.; Morales, C. A.; Shair, M. D. *J. Am. Chem. Soc.*, **2002**, *124*, 773-75.

44. Kamal, A.; Gayatri,N. L. *Tetrahedron Lett.*, **1996**, *37*, 3359-62.

45. Gingras, G. *M. Sc. thesis*, **2003**, Université Laval.

46. Yang, L.; Zhiqiang, W.; Juigping, W. *Chemistry*, **1996**, *2*, 35-37.

47. Saito, D. T.; Morimoto, M.; Akiyama, C.; Matsumoto, T.; Suzuki, K. *J. Am. Chem. Soc.*, **1995**, *117*, 10757-58.

48. Bigi, F.; Casiraghi, G.; Casnati, G.; Sartori, G. *J. Org. Chem.*, **1985**, *50*, 5018-22.

49. Nakazaki, M.; Naemura, K. *J. Org. Chem.*, **1981**, *46*, 106-11.

50. Carlson, B. W.; Miller, L. L. *J. Am. Chem. Soc.*, **1985**, *107*, 479-85.

51. Séquin-Frey, M.; Tamm, Ch. *Helv. Chim. Acta*, **1971**, *54*, 851-61.